

RR Lyrae stars in NGC 6362^{*}

R. Smolec,¹ P. Moskalik,^{1†} J. Kałużny,^{1‡} W. Pych¹ M. Różyczka,¹
and I. B. Thompson²

¹*Nicolaus Copernicus Astronomical Center of the Polish Academy of Sciences, Bartycka 18, PL-00-716 Warsaw*

²*The Observatories of the Carnegie Institution for Science, 813 Santa Barbara Street, Pasadena, CA 91101, USA*

Accepted 2017 January 1. Received 2017 January 10; in original form 2016 October 11

ABSTRACT

We present the analysis of the top-quality photometry of RR Lyrae stars in the globular cluster NGC 6362, gathered over 11 observing seasons by the CASE project. 16 stars are fundamental mode pulsators (RRab stars) and 16 are first overtone pulsators (RRc stars). In two stars, previously identified as RRab, V3 and V34, we detect additional periodicity identified as radial first overtone mode. Lower than usual period ratios (0.730 and 0.728), dominant pulsation in the radial fundamental mode and presence of a long-period modulation indicate, that these two variables are not classical RRd stars, but are new members of the recently identified class of anomalous RRd variables. In a significant fraction of RRc stars, 63 per cent, we detect additional shorter-period variability in the $(0.60, 0.65)P_1$ range. This form of double-periodic pulsation must be common in first overtone RR Lyr stars, as space observations indicate. The incidence rate we find in NGC 6362, is the highest in ground-based observations reported so far. We study the properties of these stars in detail; in particular we confirm that in the colour-magnitude diagram, this group is adjacent to the interface between RRab and RRc stars, as first reported in the analysis of M3 observations by Jurcsik et al. The incidence rate of the Blazhko effect is also very high: we observe it in 69 per cent of RRab stars and in 19 per cent of RRc stars. Rare, double-periodic modulation is reported in one RRab and in one RRc star. Finally we discuss V37 – a peculiar variable in which we detect two close high-amplitude periodicities and modulation. Its previous classification as RRc must be treated as tentative.

Key words: stars: horizontal branch – stars: oscillations – stars: variables: RR Lyrae – globular clusters: general – globular clusters: individual: NGC 6362

1 INTRODUCTION

RR Lyrae stars are low-mass, horizontal-branch, pulsating variables. They are divided into three main classes: fundamental mode, radial pulsators (RRab stars), first overtone, radial pulsators (RRc stars) and double-mode pulsators, pulsating in the radial fundamental and in the radial first overtone modes simultaneously (RRd stars). In the last few years, the top-quality photometry of RR Lyr stars gathered by the space telescopes (*MOST*, *CoRoT* and *Kepler*) and by the ground-based photometric sky surveys (e.g. Optical Gravitational Lensing Experiment, OGLE), revolutionized our knowledge about these important variables. They

can no longer be regarded as simple, radial-mode pulsators. New classes of multi-mode RR Lyr stars, that pulsate simultaneously in radial and non-radial modes, were identified. In particular in RRc and RRd stars, additional periodicities that fall in the $P_x/P_1 \in (0.60, 0.65)$ range were detected (e.g. Gruberbauer et al. 2007; Olech & Moskalik 2009; Netzel, Smolec & Moskalik 2015b, and references therein). This form of pulsation must be common among RRc/RRd stars as nearly all stars observed with the utmost precision from space do show it (14 out of 15 stars observed, e.g. Szabó et al. 2014; Moskalik et al. 2015; Molnár et al. 2015; Kurtz et al. 2016). As period ratios around 0.61 are the most common, following Jurcsik et al. (2015) we will denote the group as RR_{0.61} and the detected additional frequencies as $\nu_{0.61}$. In the recently proposed model, Dziembowski (2016) assigns the additional variability with the harmonics of non-radial modes of angular degrees 8 and 9. Non-radial modes themselves, were also detected

* Based on data obtained with du Pont and Swope telescopes at Las Campanas Observatory.

† E-mail: pam@camk.edu.pl

‡ deceased

in several of these stars (e.g. [Netzel, Smolec & Moskalik 2015b](#); [Moskalik et al. 2015](#); [Molnár et al. 2015](#), initially interpreted as period-doubling of the additional, $\nu_{0.61}$ frequencies). Another, even more puzzling group, was revealed in the OGLE photometry of RRc stars. Here, additional variability is of period longer than the first overtone period; too long to be associated with the radial fundamental mode. The period ratios tightly cluster around $P_1/P_x \approx 0.686$ ([Netzel, Smolec & Dziembowski 2015](#); [Netzel & Smolec 2016](#)). Peculiar examples of RRd stars were also discovered ([Smolec et al. 2015, 2016](#); [Jurcsik et al. 2014](#); [Soszyński et al. 2016](#)); in particular, [Soszyński et al. \(2016\)](#) identified a new class of anomalous RRd stars, characterized by anomalous period ratios, in most cases lower than in the “classical” RRd stars, by usual domination of the fundamental mode and by common presence of the modulation.

Finally, the space photometry collected by *Kepler* and *CoRoT* revolutionized our view on the Blazhko effect, a long-term quasi-periodic modulation of pulsation amplitude and/or phase (for recent reviews see e.g. [Kovács 2016](#); [Smolec 2016](#)). Although the effect is known for more than a century now, its origin remains a mystery. Detection of period doubling in a significant fraction of modulated RRab stars ([Kolenberg et al. 2010](#); [Szabó et al. 2010](#); [Benkő et al. 2014](#)) triggered the development of new models explaining the phenomenon (e.g. [Buchler & Kolláth 2011](#); [Bryant 2016](#)). The nearly continuous and top-quality photometry enabled a detailed study of the modulation on the cycle-to-cycle basis (e.g. [Guggenberger et al. 2012](#); [Le Borgne et al. 2014](#)).

The origin of the Blazhko effect or mechanisms behind the excitation of various new forms of the multiperiodic RR Lyr pulsation, remain unclear. To test the existing models (and to propose the new ones), new, top-quality observations are still needed. In particular, it is important to determine how the incidence rates and properties of the various pulsation forms depend on metallicity and on population membership of the stars. In this respect, detailed studies of globular cluster variables are crucial, but are very scarce. The only globular cluster in which dynamical properties of RR Lyr stars were studied in detail is M3 ([Jurcsik et al. 2014, 2015](#)). It is an Oosterhoff I (OoI) cluster with mean metallicity of $[\text{Fe}/\text{H}] = -1.57$ belonging to a young halo population ([Catelan 2009](#)). In this paper we analyse the photometry gathered by the Cluster AgeS Experiment (CASE) project ([Kaluzny et al. 2005](#)) for another OoI cluster with a significantly higher mean metallicity ($[\text{Fe}/\text{H}] = -0.95$), belonging to the old halo population ([Catelan 2009](#)), NGC 6362.

NGC 6362 is a nearby ($\mu_V = 14.68$ mag) globular cluster located away from the Galactic disk at $b = -17^\circ.6$ ([Harris 1996](#), 2010 edition). These properties together with a low concentration make it an attractive target for studies with ground based telescopes. Comprehensive CCD observations with 2.5-m du Pont and 1-m Swope telescopes of the Las Campanas Observatory were performed by [Mazur et al. \(1999\)](#), [Olech et al. \(2001\)](#) and [Kaluzny et al. \(2014\)](#). It was found that NGC 6362 hosts 35 RR Lyr stars, whose basic parameters were estimated by [Olech et al. \(2001\)](#) (O01 in the following) based on Fourier decomposition of light curves. The data analyzed by O01 were collected with the Swope

telescope during only one observing season, between April 17 and August 22, 1999. [Kaluzny et al. \(2014\)](#) had a much longer time-basis at their disposal, but they were mainly interested in eclipsing binaries, and left the pulsating stars untouched.

In this paper we revisit the RR Lyr stars of NGC 6362. Much longer time-base and more numerous observations than used by O01, allow us to conduct a detailed study of the dynamical properties of RR Lyr stars. Presence and properties of the Blazhko effect and excitation of additional pulsation modes, both radial and non-radial, are at the centre of our interests.

2 OBSERVATIONAL DATA AND THEIR ANALYSIS

Our paper is based on two sets of CCD images¹. The first one was obtained using the du Pont telescope and the 2048×2048 TEK5 camera with a field of view of 8.84×8.84 arcmin² and a resolution of 0.259 arcsec/pixel. Observations were conducted on 45 nights from April 21, 1995 to September 26, 2009, always with the same filters. Altogether, 1748 *V*-images were collected. The second set was obtained with the Swope telescope and the 2048×3150 SITE3 camera with a field of view of 14.8×22.8 arcmin² and a resolution of 0.435 arcsec/pixel. Observations were conducted on 103 nights from July 8, 1999 to September 9, 2009, also keeping the same filters. For the analysis, 3200 *V*-images were used. Since we are interested in the dynamical properties of RR Lyr stars, no transformation to the standard photometric system was made; we use instrumental magnitudes through the paper. We refer the interested reader to the study by O01 for the colour-magnitude diagram of the cluster, mean magnitudes and colours of the discussed RR Lyr stars, and their physical properties derived from the *V*- and *B*-band two-colour photometry through the relations given by [Simon & Clement \(1993\)](#) and [Kovács \(1998\)](#).

Our analysis is based primarily on the Swope telescope data for two reasons. First, for a given star they are typically twice as numerous as the data collected with the du Pont telescope. Second, data gathered with the du Pont telescope are of inferior quality as compared to the data gathered with the Swope telescope. Specifically, dispersion of the residuals of the Fourier fit to the du Pont data is always higher, by at least 40 per cent. As a consequence, when merging the Swope and the du Pont data the noise level in the Fourier transform increases, making the detection of weak, secondary periodicities more difficult. Lower quality of the du Pont data might be due to different reduction procedures adopted for the two telescopes: ISIS package of [Alard & Lupton \(1998\)](#) was used for the du Pont data and DIAPL package written by W. Pych² was used for the Swope data. Data from both telescopes were used together only to study period changes of RR Lyr variables. Inclusion of du Pont data allowed us to add a few additional points to the phase-change (O–C) diagrams.

¹ Data are available at the website of the CASE project, <http://case.camk.edu.pl>

² Procedures and the documentation are available at <http://users.camk.edu.pl/pych/DIAPL/index.html>

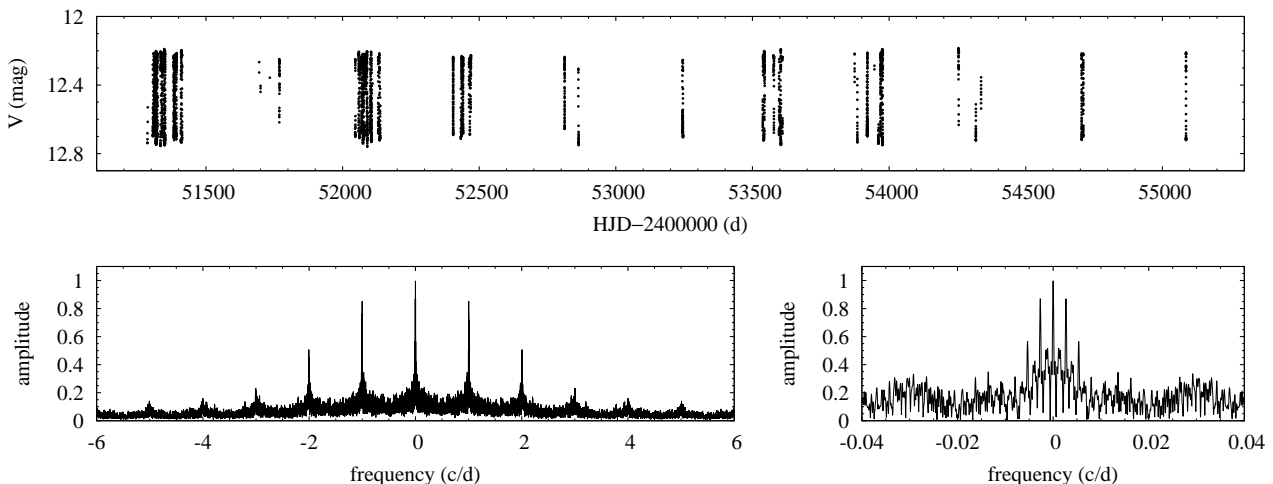


Figure 1. A typical structure of the data gathered with the Swope telescope, illustrated with the example of variable V6 (top panel). The data clearly separate into 11 observing seasons. The bottom panel shows the spectral window (bottom left), including zoom into the fine structure of 1-yr aliases (bottom right).

Typical structure of data from the Swope telescope is illustrated in the top panel of Fig. 1. The data were gathered over 11 observing seasons, below abbreviated as s1, ..., s11, clearly visible in the figure. The number of observations vary from season to season. The most extensive observations were gathered in s1 (typically ~ 1090 data points), then in s3 (~ 700 data points) and s8 (~ 400 data points). Data collected in other seasons are less numerous (between ~ 40 and ~ 300 data points). The data structure is nearly the same for all RR Lyr stars observed. The bottom panels of Fig. 1 illustrate the spectral window for data displayed in the top panel. Both daily and 1-yr aliases are very prominent and may become a source of confusion during the analysis.

Our data analysis follows the standard consecutive prewhitening technique. Significant periodicities are identified with the help of the discrete Fourier transform and included in the sine series of the following form:

$$v(t) = A_0 + \sum_i A_i \sin(2\pi\nu_i t + \phi_i), \quad (1)$$

which is fitted to the data with the help of non-linear least-square method. Amplitudes, phases and frequencies are all adjusted during the procedure. Prewhitened data are inspected for the presence of additional, lower-amplitude periodicities, which are iteratively included in eq. 1. We accept as significant periodicities with signal-to-noise (S/N) above 4; the ratio is determined from the frequency spectrum, with the noise evaluated as a mean amplitude of the Fourier transform in the $0 - 10$ c/d range. To account for the possible season-to-season zero-point differences, ten independent offset coefficients are determined during the procedure, by minimizing the dispersion of the fit (the offsets are typically below 5 mmag). Once the solution converges (no new significant signals are detected), severe outliers are removed from the data (5σ clipping).

In eq. 1 we include a few independent frequencies only. The sine series describing a typical solution contains pulsation frequency, ν , and its harmonics, $k\nu$ (below, we will use ν_0 and ν_1 for the fundamental mode and the first over-

tone frequency, respectively; at the moment, there is no need to differentiate the two). For the single-periodic and non-modulated star, these are the only terms in eq. 1, which reduces to a finite order Fourier series. Quite often, however, we detect modulation of pulsation (the Blazhko effect) or multiperiodic pulsation (or sometimes both). In the frequency spectrum, the modulation manifests as equally spaced multiplets centred at the frequency of the radial mode and its harmonics. Hence, only one independent frequency, modulation frequency, ν_m , is added to the solution. Components of the multiplet are then described as $k\nu \pm l\nu_m$. Modulation period is simply $P_m = 1/\nu_m$. Frequencies of additional periodicities, related to e.g. additional radial/non-radial pulsation modes are denoted as ν_x . Linear combinations with the dominant radial pulsation frequency, typically of the form $k\nu \pm \nu_x$, are often detected and included in the solution.

Slow phase and/or amplitude changes may occur in RR Lyr stars; in fact they are rather common in the RRc variables. Phase changes are usually most pronounced and often of irregular nature. As a result, the peaks detected at the radial mode frequency (and harmonics) are non-coherent and a residual unresolved power remains in the frequency spectrum after prewhitening. The resulting, increased noise level in the Fourier transform may hamper the detection of additional, low-amplitude periodicities. To circumvent the problem, two techniques were applied. In the first one, we simply focus on a short part of the data, either corresponding to the first season, s1, or to the first four seasons, s1-s4. On a shorter time scale, the phase changes are not that disruptive. The second technique we apply is a time-dependent prewhitening. The details of the method and its application to quasi-continuous *Kepler* data are discussed in Moskalik et al. (2015), the Appendix. In Netzel, Smolec & Moskalik (2015a) the technique was applied to seasonal, ground-based data and here we follow the same approach. In a nutshell, the data are first divided into seasons, and amplitudes and phases are determined for each season separately. Then, the data are prewhitened with the

sine series of the form displayed in eq. 1, except that amplitudes and phases are now season-dependent. The procedure filters out possible amplitude/phase variations on a time scale longer than the typical length of the observing season. The frequency spectrum is cleaned from the unresolved power and the overall noise level drops, enabling detection of additional low-amplitude periodicities. Because of scarce data in some of the observing seasons, the technique can in most cases be applied to five seasons only (s1, s3, s4, s7 and s8).

Whenever these techniques appeared crucial for the detection of additional phenomena (modulation, additional periodicities) we explicitly state so while discussing a given star.

3 RESULTS

3.1 Overview

We have analysed photometric data for 35 pulsators from NGC 6362, all of which were identified as RR Lyr stars in the study of O01 and earlier studies of the cluster summarized there. Of these, 18 were classified as RRab and 17 as RRc variables. For the majority of stars we confirm the classification of O01, with the exception of V3, V34 and V37. In the first two stars, previously classified as RRab, we detect the first overtone, and now classify them as RRd variables; in fact they are new members of the anomalous RRd class identified recently by [Soszyński et al. \(2016\)](#), as we discuss in detail in Section 4.2. In addition, V37, classified by O01 as RRc, is discussed separately in our study (Section 3.7). Most likely, V37 is not RR Lyr star, but a pulsating variable of different nature. The basic properties of 16 RRab and 16 RRc variables are collected in Tab. 1 (which also contains data on V37 in the last row). These include pulsation period and pulsation amplitude as well as information about additional phenomena detected in the stars (the last column). The phenomena are: Blazhko modulation ('BL' in the last column), double-periodic Blazhko modulation ('2×BL') and the presence of the additional, non-radial pulsation ('nr'). All 11 seasons of Swope data were used to derive pulsation periods and amplitudes given in Tab. 1 and hence, these quantities are means over the time span of the observations. This comment is particularly relevant for the RRc stars, where we often detect fast and irregular period changes (see Section 3.4).

In Fig. 2 we present the period-amplitude diagram for the discussed stars, which nicely confirms the adopted mode classification. For the two RRd stars, data corresponding to the dominant fundamental mode are used in this plot. Colour-magnitude diagram is presented in Fig. 3. For this plot we used the standard *V* and *B*-band mean brightness from O01 (their tab. 1). A separation of RRc from RRab variables is rather clear. Of the two newly identified RRd stars, V3 is located in the colour-magnitude plot in between RRc and RRab stars. V34 appears a bit cooler, but its location does not arise suspicions. Further support for the adopted mode classification is presented in Fig. 4, which presents low-order Fourier decomposition parameters for all the discussed variables. RRab and RRc stars clearly separate in these plots. The two RRd stars, with dominant pulsation

Table 1. Basic properties of the analysed RRab and RRc variables: star's id, type, pulsation period and Fourier amplitude, i.e. A_i from eq. 1 at the fundamental/first overtone frequency. All numbers are given to the last significant digit. In the last column remarks are given: 'BL' – Blazhko effect detected, '2×BL' – double-periodic Blazhko effect detected, 'nr' – non-radial mode(s) detected. Properties of the two RRd stars are listed separately in Tab. 4.

id	type	P (d)	A (mag)	remarks
V1	RRab	0.50479162	0.3667	BL
V2	RRab	0.488973010	0.4143	
V5	RRab	0.52083783	0.3039	BL
V7	RRab	0.521581388	0.3592	BL
V12	RRab	0.5328814	0.3285	BL
V13	RRab	0.58002740	0.3556	BL
V16	RRab	0.525674215	0.3458	
V18	RRab	0.51288484	0.3429	BL
V19	RRab	0.59450528	0.2080	
V20	RRab	0.69835898	0.1535	BL
V25	RRab	0.455890887	0.4195	
V26	RRab	0.60217449	0.2132	
V29	RRab	0.64778329	0.1687	BL
V30	RRab	0.61340457	0.3241	2×BL
V31	RRab	0.60021294	0.2211	BL
V32	RRab	0.49724171	0.3759	BL
V6	RRc	0.26270671	0.2226	2×BL
V8	RRc	0.38148471	0.2023	nr
V10	RRc	0.265638816	0.2222	BL
V11	RRc	0.288789268	0.2433	
V14	RRc	0.24620647	0.1587	
V15	RRc	0.279945707	0.2194	nr
V17	RRc	0.31460473	0.1995	nr
V21	RRc	0.281390043	0.2366	nr
V22	RRc	0.26683523	0.2304	
V23	RRc	0.275105063	0.2428	nr
V24	RRc	0.32936190	0.2218	nr
V27	RRc	0.27812399	0.2402	nr
V28	RRc	0.3584133	0.1898	
V33	RRc	0.30641758	0.2007	nr
V35	RRc	0.29079074	0.2098	nr
V36	RRc	0.31009148	0.1790	nr, BL
V37	?	0.25503903	0.1174	BL

in the fundamental mode, fit within the RRab group (no harmonics are detected for the first overtone, consequently, the corresponding Fourier parameters cannot be computed). In Figs. 5 and 6 we present a gallery of phased light curves of RRab and RRc variables, respectively. Stars are sorted by the increasing pulsation period (given in each panel). Note that for all stars, data from all 11 seasons were used in the plots. For some stars the Blazhko modulation is obvious (e.g. in V5 and V31, which are of RRab type, or in V6 and V10, which are of RRc type). In others, particularly in several RRc stars, the data do not phase well, but form a band of light curves shifted in phase (e.g. V8, V14, V24, V28). The bands are due to period changes in these stars. The most extreme case is V28.

In the following Sections, we first discuss RRab variables (Section 3.2 and 3.3), then RRc stars (Section 3.4 and 3.5), two RRd pulsators (Section 3.6) and finally the odd-ball, V37 (Section 3.7).

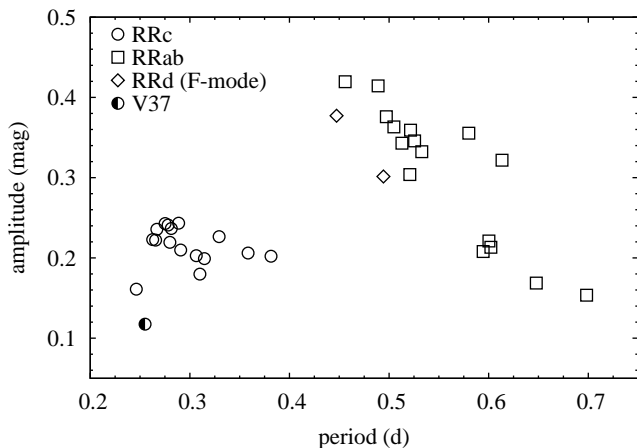


Figure 2. Period-amplitude diagram for RR Lyrae stars of NGC 6362. Note that Fourier amplitudes are used in the plot.

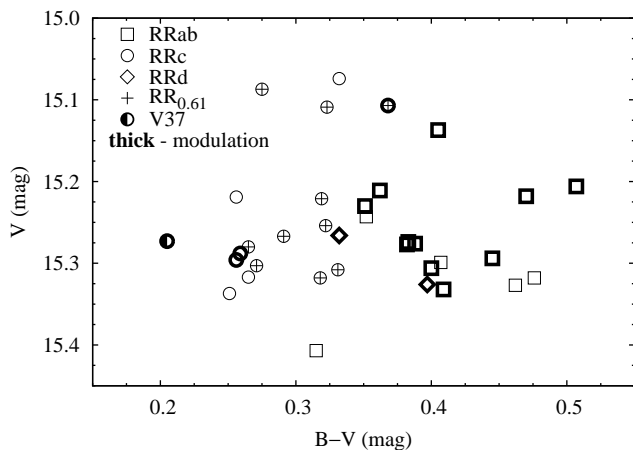


Figure 3. Colour-magnitude diagram for RR Lyrae stars of NGC 6362. Standard magnitudes and colours were adopted from O01.

3.2 RRab stars

Altogether, NGC 6362 hosts 16 RRab stars; their basic properties are given in Tab. 1, and phased light curves are presented in Fig. 5.

Eleven variables show the Blazhko modulation, which was recognized based on the analysis of the frequency spectrum. For some stars however, the effect is obvious already from the analysis of the phased light curve (see e.g. V5, V7, V13 or V31 in Fig. 5). The prewhitening sequence is illustrated with the example of variable V5 which shows clear, large-amplitude modulation of pulsation with a period of about 56.2 d. Fig. 7 shows a large section of the frequency spectrum of V5 covering the first five harmonics (left-most column), and zooms into smaller sections: around modulation frequency (second column), centred at ν_0 (third column) and centred at $6\nu_0$ (last column). The top row in Fig. 7 illustrates the frequency spectrum after prewhitening with the fundamental mode frequency and its harmonics. A triplet at ν_0 is apparent, with a higher amplitude side peak on the low-frequency side of ν_0 . The following rows of Fig. 7 show the prewhitening process, first with triplet components (second, third and fourth rows), and finally with all signifi-

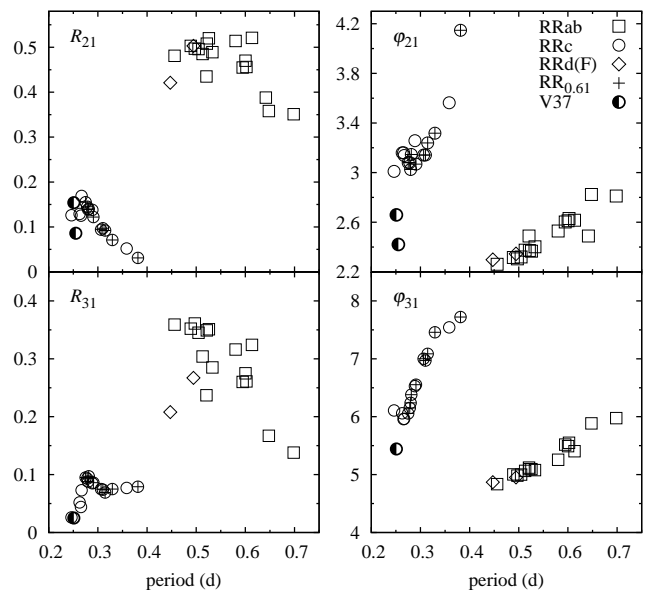


Figure 4. Low-order Fourier decomposition parameters for pulsating stars of NGC 6362.

cant quintuplet components, which are more pronounced at higher order harmonics of the fundamental mode. Quintuplets are incomplete; only negative frequency components, i.e., $k\nu_0 - 2\nu_m$, are significant. We also note that in the low frequency range, peaks at the modulation frequency and twice the modulation frequency are prominent (second column in Fig. 7). After prewhitening with the fundamental mode frequency, its harmonics, and all multiplet components no additional significant power is detected in the frequency spectrum (bottom row of Fig. 7).

The top section of Tab. 2 summarizes the basic properties of the Blazhko modulation in RRab stars of NGC 6362. These are: modulation period, P_m , amplitudes of the lower (A_-) and higher (A_+) frequency side peaks at ν_0 , relative amplitude of modulation, i.e. $A_{\text{mod}} = \max(A_-, A_+)/A$, the asymmetry parameter defined by Alcock et al. (2003) as, $Q = (A_+ - A_-)/(A_+ + A_-)$, indication which data were used in the analysis ('data' column) and some details on the main modulation components detected in the spectrum.

In all but one modulated RRab stars only a single modulation period was found. It varies from ≈ 17 d (V1, V32) to ≈ 82 days (V31). Two modulation periods were identified in V30, ≈ 34.8 d and ≈ 216.4 d. The relative modulation amplitude vary from ≈ 3 per cent (V30, V32) to ≈ 24 per cent (V5). Clear modulation triplets were detected in the majority of stars, with the exception of V12 and V20, in which only close doublets were detected at $k\nu_0$. Complete quintuplets or components of the quintuplets were detected in V1, V5, V13 and V29. V29 is an interesting case. No additional side peaks were detected on the low frequency side of $k\nu_0$, however side peaks with $+\nu_m$ and $+2\nu_m$ separation appear on the high frequency side of $k\nu_0$. In addition, starting from $2\nu_0$, the $+2\nu_m$ components are significantly higher than the $+\nu_m$ components. Thus, incomplete and strongly asymmetric quintuplets are detected in V29. Finally, in V13 we detect one significant component of septuplet, $10\nu_0 - 3\nu_m$. In four stars, in the low-frequency range we detect significant peaks

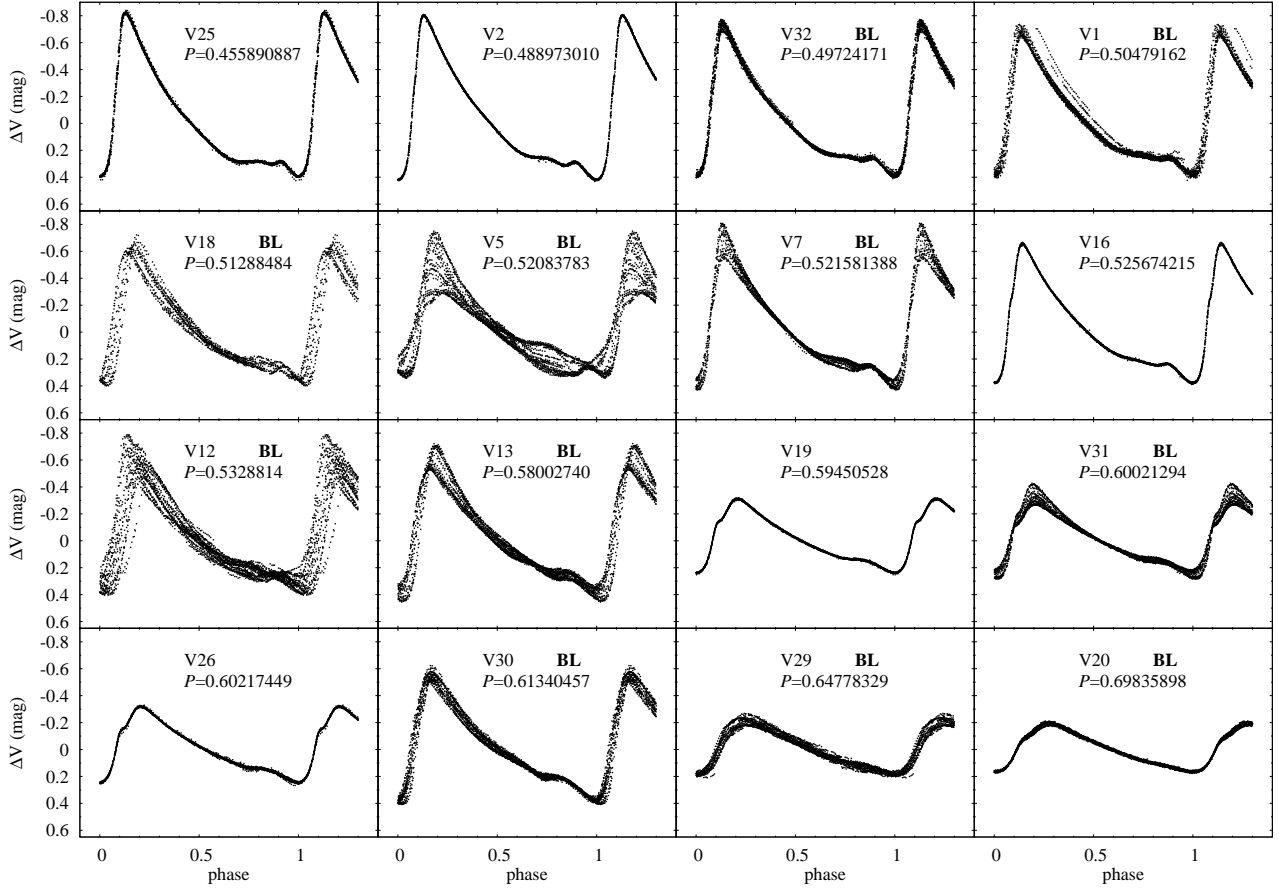


Figure 5. A collection of phased light curves for all observed RRab stars, sorted by the increasing pulsation period. Data from all 11 observing seasons were used for each star. The adopted pulsation period is given in each panel, together with information about possible modulation (BL).

at the modulation frequency (V5, V7, V13, V31) and at its harmonic (V5, V13).

V30 is an interesting and rare case of RRab star with two modulation periods. The modulation with the shorter period is dominant – the relative modulation amplitude is 7.5 per cent, to be compared with 2.5 per cent for the modulation with the secondary, longer period. For both modulation periods, clear triplet structures are detected at $k\nu_0$.

We note that O01 did not analyse the Blazhko effect in RRab stars of NGC 6362 in any detail. Based on the light curve scatter, V5, V7, V12, V13 and possibly V18, were regarded as stars showing the Blazhko effect. A further discussion on the Blazhko effect in NGC 6362 is postponed to Section 4.1.

With the exception of V25 (see Section 3.3 below) no additional periodicities that could be associated with other radial or non-radial modes of pulsation were detected in RRab stars.

3.3 Notes on individual RRab stars

V16 – in the analysis of all data, after prewhitening with the fundamental mode frequency and its harmonics, we detect significant ($S/N \approx 5$) remnant power at $k\nu_0$ in the form of several closely spaced peaks of similar height, which may be due to a long-period modulation. The period would be either

≈ 1070 d or ≈ 576 d, depending which of the 1-yr aliases is chosen. Although these are formally resolved, the frequency spectrum at $k\nu_0$ corresponds to a wide power excess rather than to a genuine modulation and may result from irregular amplitude and/or phase changes. In addition, after applying the time-dependent prewhitening to the data of the most numerous seasons (s1, s3, s4, s7 and s8) no additional power is detected at the fundamental mode and its harmonics. Consequently, we do not regard V16 as Blazhko variable.

V25 – in the analysis of all data, the fundamental mode and its harmonics are non-coherent – a strong remnant power remains at $k\nu_0$ after prewhitening. Interestingly, when we analyse the first four seasons only, the effect disappears: the fundamental mode and its harmonics are coherent and no remnant power is present. This suggests a possible significant period change/jump during the observations. In the residuals of the s1–s4 data we detect an additional periodicity ($S/N = 6.1$) of long period, $P_x = 1.03503$ d, $P_x/P_0 = 2.2704$. This periodicity cannot correspond to any acoustic mode of oscillation. No combination frequencies with the radial mode are detected. In addition, we note that a signal of nearly the same frequency is detected also in two other stars, in V10 and in V11 (see Section 3.5). Consequently, this signal cannot be intrinsic to the stars, but is most likely an artefact (origin of which remains unknown).

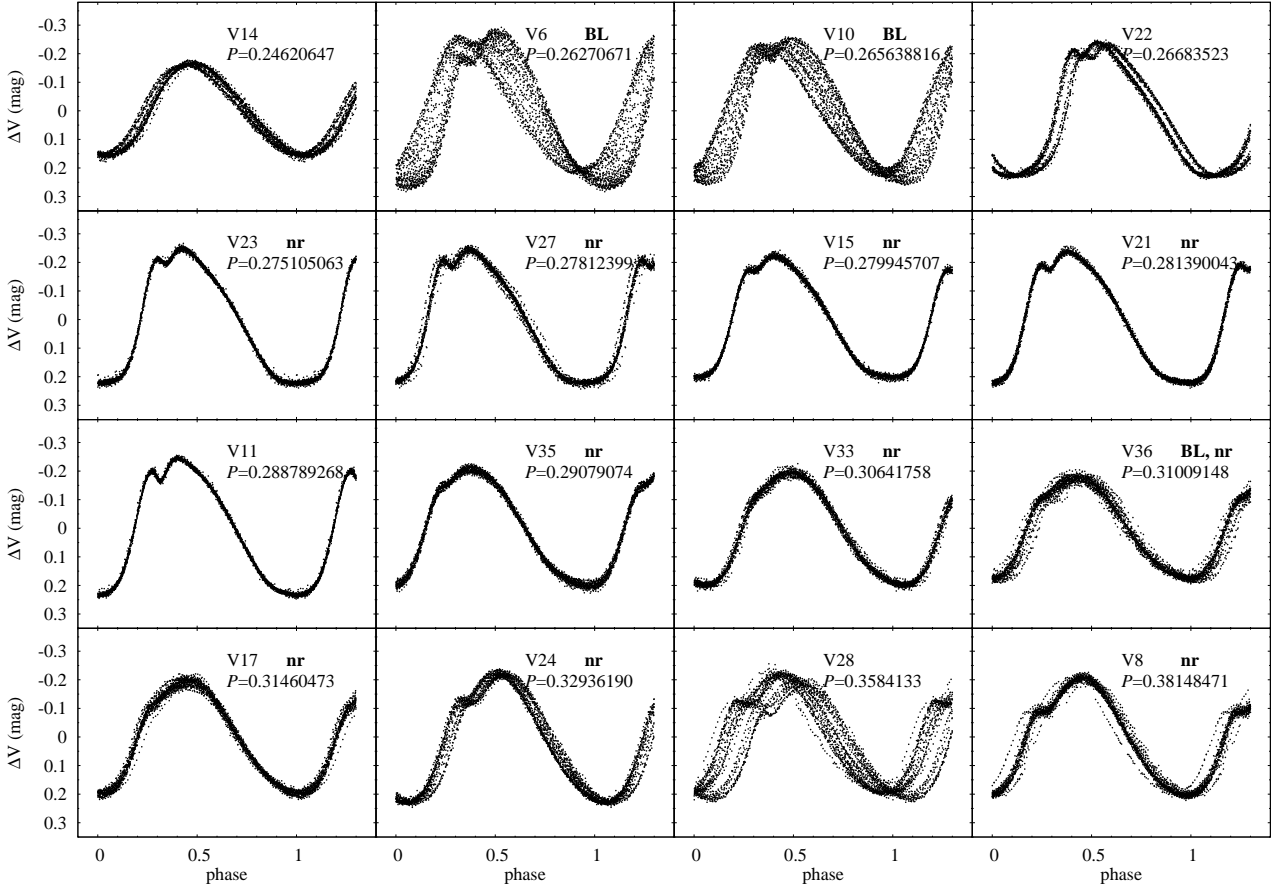


Figure 6. A collection of phased light curves for all observed RRc stars, sorted by the increasing pulsation period. Data from all 11 observing seasons were used for each star. The adopted pulsation period is given in each panel, together with information about possible modulation (BL) or about presence of additional non-radial pulsation (nr).

V2, V19 and V26 – these stars are genuine, single-periodic RRab variables, without any sign of modulation or additional periodicities in the frequency spectrum.

3.4 RRc stars

Altogether, NGC 6362 hosts 16 genuine RRc stars; their basic properties are given in Tab. 1, and phased light curves are presented in Fig. 6. V37, previously classified as RRc, is discussed separately in Section 3.7.

The most interesting result is the detection of additional periodicities in the $P/P_1 \in (0.60, 0.65)$ range in 10 out of 16 RRc stars. These are new members of the RR_{0.61} class, described in the Introduction. Data on all RR_{0.61} stars are collected in Tab. 3, in which we report: period of the additional variability, P_x , period ratio with the first overtone period, and amplitude of the additional variability, A_x . This amplitude is always low, in the mmag range (the highest amplitude is ≈ 5 mmag in V17), which makes the detection of additional variability challenging. This is particularly true for stars in which strong phase changes are present. In such a case, after prewhitening with the first overtone frequency and its harmonics, residual power remains in the frequency spectrum and the overall noise level in the Fourier transform is increased. This hampers the detection of the possible secondary signal. For such stars we can circumvent the prob-

lem, either by selecting a shorter data subset, so the period change is not as pronounced, or by applying time-dependent prewhitening. In the former case, we select either the first season (s1), or the first four seasons (s1-s4). That way we include the most densely sampled seasons s1, s3 and s4 (see Fig. 1) which guarantees the lowest noise level in the Fourier transform. Sixth column of Tab. 3 explicitly identifies which data were used in the analysis. Time-dependent prewhitening was applied for three stars ('tdp' in the last column of Tab. 3).

The detections are illustrated in Fig. 8 for three stars, V15, V33 and V17, in the top, middle and bottom rows, respectively. The left panels show large sections of the frequency spectrum after prewhitening with the first overtone frequency and its harmonics. Additional, significant signals are clearly detected between ν_1 and $2\nu_1$. The right panels of Fig. 8 show zooms into the interesting part of the spectrum. For V15 a power excess of a complex structure is well visible. After prewhitening with the frequency of the highest peak, located at $P_x/P_1 \approx 0.613$, close significant peaks still remain in the spectrum. For V33 (middle row of Fig. 8), after prewhitening with the highest peak located at $P_x/P_1 \approx 0.613$ (marked with an arrow), another, well separated peak becomes significant (at $P_x/P_1 \approx 0.631$, also marked with an arrow). In the case of V17 (bottom row of Fig. 8), three well separated peaks are detected (cen-

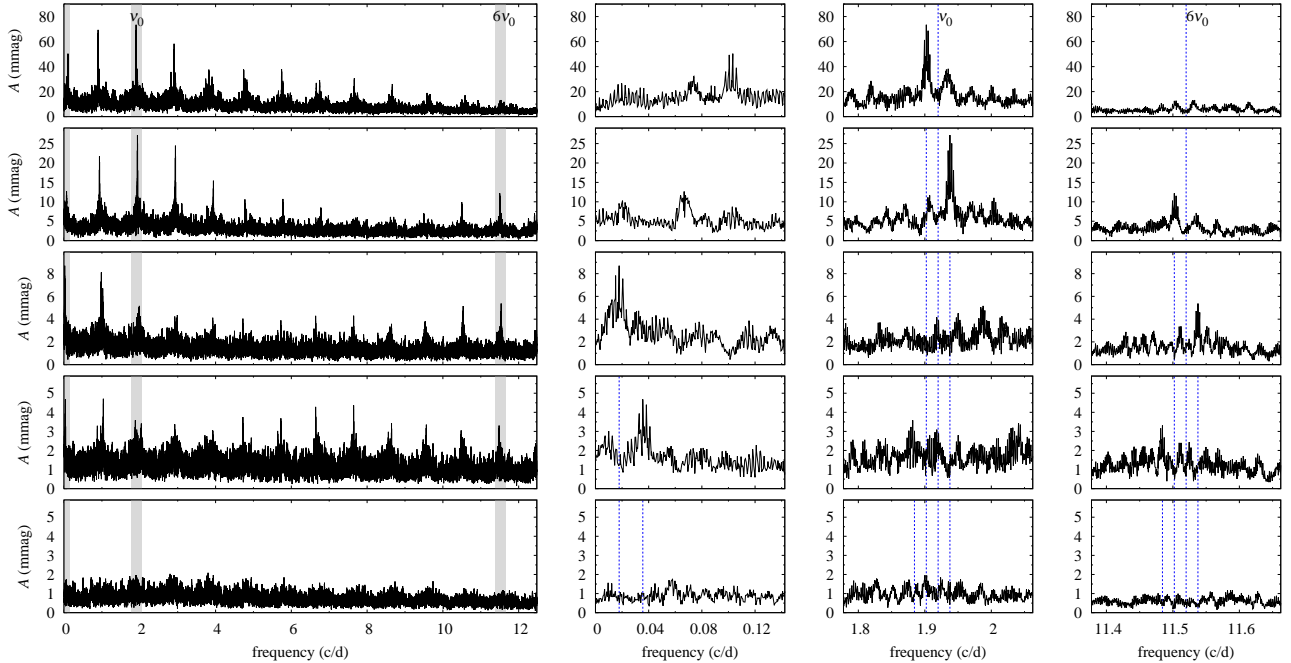


Figure 7. Prewhitening sequence for Blazhko RRAb variable V5. The first column shows the wide frequency range, up to $6.5\nu_0$. The next columns show zooms into three grey-shaded regions: at a low frequency range, at a range centred at ν_0 , and at a range centred at $6\nu_0$. Consecutive rows show, from top to bottom: (*first row*) frequency spectrum after prewhitening the fundamental mode and its harmonics; (*second*) in addition $k\nu_0 - \nu_m$ for $k = 1, \dots, 5$ were prewhitened; (*third*) in addition $k\nu_0 - \nu_m$ for $k = 6, \dots, 10$ and $k\nu_0 + \nu_m$ for $k = 1, \dots, 5$ were prewhitened; (*fourth*) all significant triplet components and the significant peak at ν_m were prewhitened; (*fifth*) all significant quintuplet components and the significant peak at $2\nu_m$ were prewhitened. Except the first-column plots, prewhitened frequencies are marked with dashed lines.

tred at $P_x/P_1 \approx 0.612, 0.622$ and 0.631). V17 and V33 are the only stars in which more than one peak is reported in Tab. 3. These peaks correspond to two (V33) or three (V17) sequences formed by RR_{0.61} stars in the Petersen diagram (see the discussion in Section 4.3). For other stars, only one entry is present in Tab. 3. This doesn't mean that the corresponding peak is coherent. Typically, the detected peak has a complex structure, similar to that illustrated for V15 in the top panel of Fig. 8. In all such cases, only the frequency and amplitude of the highest peak is reported in Tab. 3. The described, complex appearance of additional periodicities in the frequency spectrum is common for this class of stars, as we discuss in more detail in Section 4.3.

Another interesting phenomenon, detected in three RRc stars, V6, V10 and V36, is the Blazhko effect. Basic properties of the modulation are given in the bottom section of Tab. 2. Modulation periods are significantly shorter than those observed in RRAb stars; the longest is only ≈ 15.5 days (V6), while the shortest modulation period is ≈ 8.5 d (V10). In all three stars the modulation side peaks on higher frequency side of ν_1 are higher; although for V6 and V10 the two detected triplet components are of comparable height.

There is no doubt that a genuine modulation is observed in V6 (with P_{m1}) and in V10. In both cases at least one complete quintuplet is observed at the harmonics of the first overtone frequency. Admittedly, the secondary modulation in V6 and modulation in V36 are less firmly established. Although in both cases we detect a significant side peak on the higher frequency side of the first overtone frequency, it is the

only additional signal detected in the frequency spectrum, i.e. no additional modulation side peaks are identified.³

We note that V36 shows the Blazhko effect and $\nu_{0.61}$ periodicity, simultaneously. Further discussion of the Blazhko effect and of RR_{0.61} stars in NGC 6363 is in Section 4.1 and 4.3, respectively.

Nearly all RRc stars show significant period changes over the time-span of the analysed observations (11 yrs). It is well visible in Fig. 6 as majority of the light curves cannot be phased well with a single period. To study the period changes in more detail, we used together data from both Swope and du Pont telescopes. For each star and for both data sets we fixed the same initial epoch and the same period (at which all data analysed simultaneously phase best). Then we analysed the phase (ϕ_1) and amplitude (A_1) variation on the season-to-season basis. We note that phase change diagrams are equivalent to O–C diagrams. Only for V10, V15 and V23 phase changes are rather small and insignificant. In other stars more complex patterns are observed which we illustrate in Fig. 9. V33 is the only clear case in which the overall phase change can be modelled with a quadratic function. Such a phase change corresponds to a linear period increase at a rate of $\dot{P} = 0.71 \text{ d Myr}^{-1}$. This is

³ We also note that the two modulation periods are the same within the resolution of the data. The same modulation periods and similar appearance of the side peaks in the frequency spectrum (on the positive side of ν_1) may suggest an artificial origin of this modulation in the two stars; however it is hard to postulate any reasonable cause of such an artefact.

Table 2. Properties of the Blazhko variables. Consecutive columns contain: star’s id, type, pulsation period, modulation period, amplitudes of the modulation side peaks located near the basic pulsation frequency, at lower (A_-) and at higher frequency (A_+), relative modulation amplitude, A_{mod} , and asymmetry parameter, Q . Results are based on the analysis of data indicated in the 9th column. The last column lists the main modulation side peaks detected in the frequency spectrum.

id	type	P (d)	P_m (d)	A_- (mag)	A_+ (mag)	A_{mod}	Q	data	main modulation components
V1	RRab	0.50479165	17.4043	0.0065	0.0182	0.050	0.477	s1-s4	$\pm\nu_m$ components at $\nu_0, \dots, 7\nu_0$; $+\nu_m$ components at $8\nu_0, \dots, 10\nu_0$; $+2\nu_m$ components at $3\nu_0, 5\nu_0$ and weak at $6\nu_0$
V5	RRab	0.52083783	56.190	0.0723	0.0307	0.238	-0.404	all	ν_m ; $2\nu_m$; $\pm\nu_m$ components at $\nu_0, \dots, 7\nu_0$, $9\nu_0, 10\nu_0$; $-\nu_m$ components at $8\nu_0, 11\nu_0$; $-2\nu_m$ components at $3\nu_0, \dots, 10\nu_0$
V7	RRab	0.521581388	41.191	0.0239	0.0143	0.067	-0.253	all	ν_m ; $\pm\nu_m$ components at $\nu_0, \dots, 13\nu_0$; $+\nu_m$ components at $14\nu_0, \dots, 19\nu_0, 21\nu_0, 22\nu_0$
V12	RRab	0.53286906	57.710	0.0548	-	0.164	-1.000	s1-s4	$-\nu_m$ components at $\nu_0, \dots, 8\nu_0$
V13	RRab	0.58002740	35.2368	0.0344	0.0320	0.097	-0.036	all	ν_m ; $2\nu_m$; $\pm\nu_m$ components at $\nu_0, \dots, 9\nu_0$; $-\nu_m$ component at $10\nu_0$; $\pm 2\nu_m$ components at $4\nu_0, \dots, 8\nu_0$; $-2\nu_m$ components at $9\nu_0, \dots, 13\nu_0$; $+2\nu_m$ components at $2\nu_0, 3\nu_0$; $-3\nu_m$ component at $9\nu_0, \dots, 13\nu_0$
V18	RRab	0.51288484	78.036	0.0286	0.0486	0.142	0.259	all	$\pm\nu_m$ components at $\nu_0, \dots, 6\nu_0$; $+\nu_m$ components at $7\nu_0, 8\nu_0$
V20	RRab	0.69835898	73.332	-	0.0089	0.058	1.000	all	$+\nu_m$ components at $\nu_0, \dots, 5\nu_0$
V29	RRab	0.64778329	66.917	-	0.0209	0.124	1.000	all	$+\nu_m$ components at $\nu_0, \dots, 3\nu_0$; $+2\nu_m$ components at $2\nu_0, \dots, 4\nu_0$;
V30	RRab	0.61340457	34.809	0.0241	0.0109	0.074	-0.376	all	$\pm\nu_{m1}$ components at $\nu_0, \dots, 6\nu_0$; $-\nu_{m1}$ component at $7\nu_0$
			216.37	0.0066	0.0081	0.025	0.101		$\pm\nu_{m2}$ components at $\nu_0, \dots, 5\nu_0$; $+\nu_{m2}$ component at $6\nu_0$
V31	RRab	0.60021294	82.267	0.0191	0.0133	0.086	-0.179	all	ν_m ; $\pm\nu_m$ components at $\nu_0, \dots, 16\nu_0$, $18\nu_0, \dots, 20\nu_0$; $+\nu_m$ components at $17\nu_0, 21\nu_0$
V32	RRab	0.49724171	17.3010	0.0053	0.0119	0.032	0.384	all	$\pm\nu_m$ at ν_0 ; $+\nu_m$ components at $2\nu_0, \dots, 12\nu_0$
V6	RRc	0.26270529	15.4504	0.0610	0.0624	0.280	0.012	s1-s4	$2\nu_{m1}$; $\pm\nu_{m1}$ components at $\nu_1, \dots, 6\nu_1$; $+\nu_{m1}$ component at $8\nu_1$; $\pm 2\nu_{m1}$ components at $2\nu_1, 4\nu_1, \dots, 7\nu_1$; $-2\nu_{m1}$ component at $3\nu_1$
			13.771	-	0.0033	0.015	1.000		$+\nu_{m2}$ at ν_1
V10	RRc	0.265638816	8.52242	0.0429	0.0544	0.245	0.118	all	ν_m ; $2\nu_m$; $\pm\nu_m$ components at $\nu_1, \dots, 7\nu_1$; $+\nu_m$ component at $8\nu_1$; $\pm 2\nu_m$ component at $2\nu_1$; $-2\nu_m$ components at $3\nu_1, \dots, 5\nu_1$
V36	RRc	0.310084	13.764	-	0.0036	0.020	1.000	s1	$+\nu_m$ at ν_1

two orders of magnitude faster than expected due to the stellar evolution, see e.g. [Catelan \(2009\)](#). We also note that the fit for V33 is not perfect; residuals are significant, and indicate possible more complex period changes on a shorter time scale. In all other stars more complex phase changes are apparent, examples are V11, V14 and V28 in Fig. 9. The phase changes occur on a relatively short time-scale and are not parabolic. Such phase changes are of non-evolutionary character and are commonly observed in first overtone pulsators, both RR Lyr stars and classical Cepheids (e.g. [Szeidl et al. 2011](#); [Poleski 2008](#)). Interesting phase changes are detected for V21 and V22, as they might be periodic, with periods of order of ~ 2600 d. A longer time-base of observations is needed for a confirmation, however.

For all stars we also investigated the amplitude stability. In contrast to the pulsation phases, the amplitudes are stable in most cases (with the exception of Blazhko variables). Only in a few stars the changes appear significant but the variation is below 5 per cent.

A study of period changes in RRab stars of NGC 6362 is more difficult because of the strong Blazhko modulation in the majority of these variables. Analysis for stars without the Blazhko modulation shows no or negligible phase changes. For Blazhko variables, periods must also be stable as in the majority of cases we find no remnant power at $k\nu_0$ after prewhitening (see however Section 3.3 and notes on V16 and V25). Also, a comparison of light curves displayed in Figs. 5 and 6 clearly shows, that in contrast to the RRc stars, in the RRab stars periods are very stable – in all cases data can be phased well with a single period.

3.5 Notes on individual RRc stars

V8 – the additional non-radial mode detected in this star, reported in Tab. 3, is weak ($S/N = 3.8$); however, the presence of the combination frequency, $\nu_1 + \nu_x$, supports the detection. In addition we detect a significant ($S/N = 5.5$) periodicity at $P_{x2} = 0.47427$ d ($A_{x2} = 5.6$ mmag), so $P_1/P_{x2} = 0.8043$.

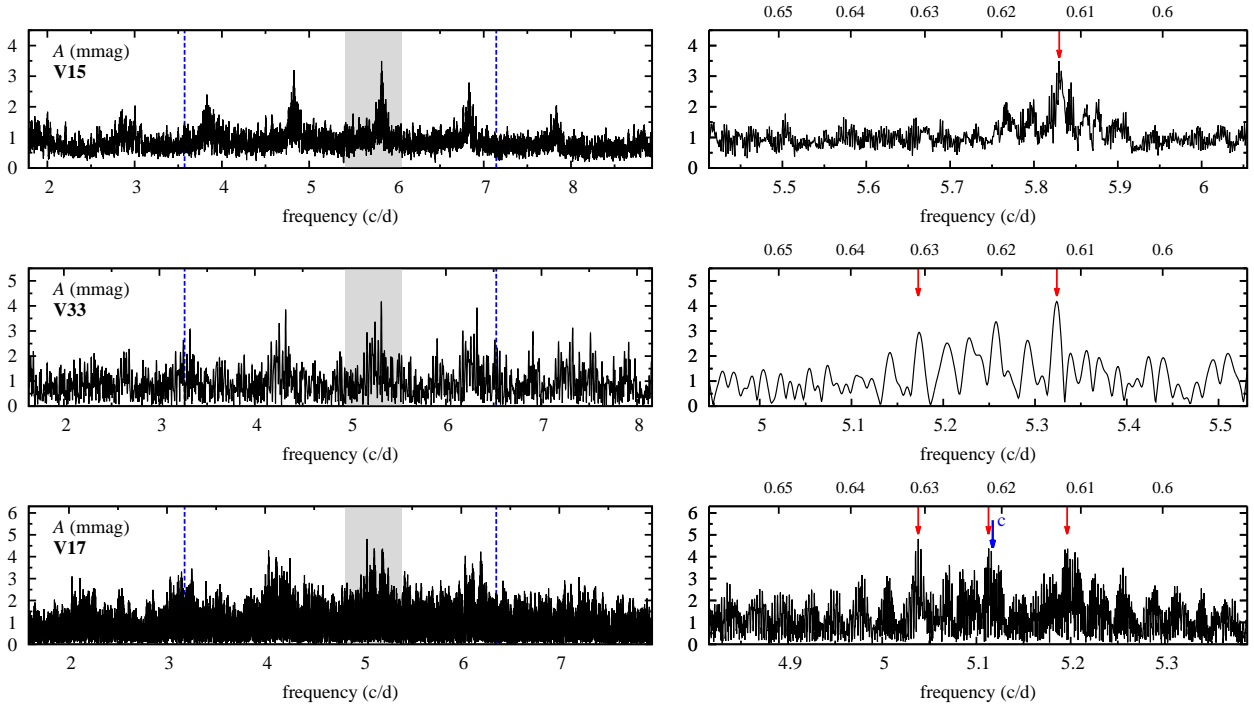


Figure 8. Detection of additional periodicities in three RRc stars, V15, V33 and V17. Left panels show the frequency spectrum in the $(0.5\nu_1, 2.5\nu_1)$ range, prewhitened with the first overtone frequency and its harmonics (dashed lines). Right panels show zoom into the frequency range with additional peaks, marked with grey-shaded box in the left panels. Detected peaks are marked with arrows. At the top axis of right panels, period ratio scale, P/P_1 is plotted.

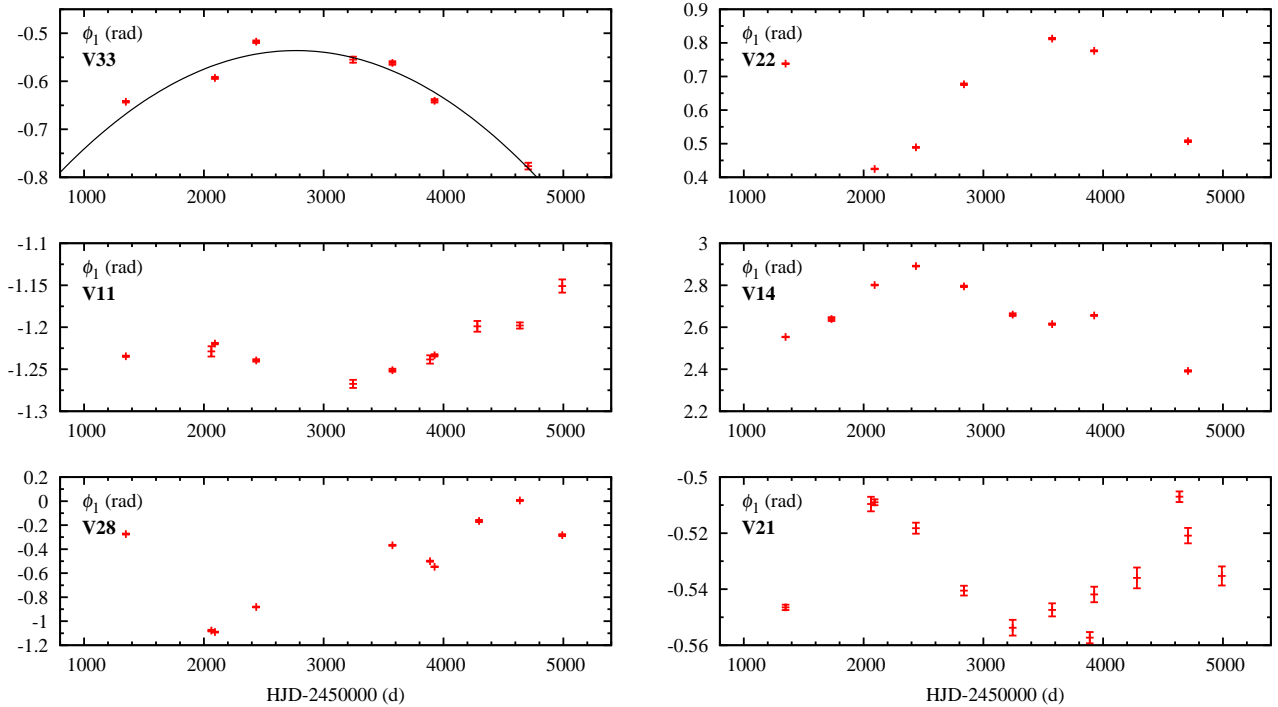


Figure 9. Phase changes in 6 RRc stars over 11 observing seasons.

Table 3. RRc stars with an additional shorter period variability in the $P_x/P_1 \in (0.60, 0.65)$ range. Consecutive columns contain: star's id, first overtone period, P_1 , additional period, P_x , period ratio, P_x/P_1 , amplitude of the additional periodicity, A_x , and indication which data were used in the analysis. Remarks in the last column: 'c' – combination frequency, $\nu_1 + \nu_x$ detected, 'a' – complex appearance of $\nu_{0.61}$ signal (e.g. non-coherent, additional close peaks, broad power excess), 'tdp' – time-dependent prewhitening used in the analysis, P_1 determined from s1., 'p' – additional periodicity detected in the star; see Section 3.5 for details.

id	P_1 (d)	P_x (d)	P_x/P_1	A_x (mag)	data	remarks
V8	0.3814813	0.23975	0.6285	0.0026	s1	c (weak), p
V15	0.279945707	0.1715296	0.6127	0.0034	all	a
V17	0.31460523	0.1924287	0.6117	0.0049	s1-s4	
		0.1955796	0.6217	0.0045		
		0.1984814	0.6309	0.0045		
V21	0.281390043	0.1730099	0.6148	0.0033	all	a
V23	0.275105063	0.1688913	0.6139	0.0023	all	c, a
V24	0.3293664	0.2002600	0.6080	0.0026	all	tdp
V27	0.2781221	0.1707740	0.6140	0.0024	all	a, tdp
V33	0.3064223	0.187836	0.6130	0.0047	s1	
		0.19332	0.6309	0.0037		
V35	0.29079074	0.1783040	0.6132	0.0029	all	a, p
V36	0.310084	0.1897573	0.6120	0.0032	all	tdp

Such a period ratio is expected for double-mode first and second overtone pulsator, but only if the additional, weak periodicity corresponds to the first overtone and the dominant variability to the second overtone. We judge such possibility unlikely. Consequently, additional long-period variability may be due to a g-mode oscillation or to a contamination.

V10 – in the data prewhitened with the first overtone frequency, its harmonics and all detected modulation side peaks, we found an additional significant ($S/N = 4.9$) periodicity, $P_x = 1.03510$ d. This is most likely an artefact, as we detect signals of nearly the same frequency in two other stars, *V25* and *V11*.

V11 – in the most numerous seasonal dataset, s1, after prewhitening with the first overtone frequency and its harmonics we detect an additional significant ($S/N = 5.3$) long-period variability, $P_x = 1.0363$ d. This periodicity cannot correspond to any acoustic mode of oscillation. This is most likely an artefact, as we detect signals of nearly the same frequency in two other stars, *V10* and *V25*.

V35 – in addition to a non-radial mode detected in this star (Tab. 3) another long-period variability is also present, $P_{x2} = 0.520838$ d ($A_{x2} = 3.6$ mmag, $S/N = 4.8$). The period ratio is $P_1/P_{x2} = 0.5583$. No combination frequencies are detected. The additional variability cannot correspond to acoustic mode of oscillation. It may be due to a g-mode oscillation or to a contamination.

V14, *V22* and *V28* – except that in all cases period changes are detected (which is well visible already in Fig. 6) we find no signature of modulation or of additional modes in these stars.

3.6 RRd stars

Two stars previously identified as of RRab type, *V3* and *V34*, are in fact RRd pulsators. These are first RRd stars identified in NGC 6362. Light curves phased with the fundamental mode period, presented in Fig. 10, show a significant scatter, which is mostly due to the long-period modulation of the fundamental mode, discussed later on in this section. In

both stars, an additional significant shorter-period variability is detected. Fig. 11 illustrates the detection for both variables. It shows frequency spectra after prewhitening with the fundamental mode frequency, its harmonics and all significant modulation components. Additional, very prominent, signals are marked with arrows. Combination frequencies are detected as well, and are also marked in Fig. 11 with arrows. Period ratios with the fundamental mode period, 0.7304 and 0.7275, for *V3* and *V34*, respectively, suggest that the additional variability corresponds to the radial first overtone. The period ratios are in fact lower than typically observed in RRd stars of similar fundamental mode period. *V3* and *V34* are new members of the *anomalous RRd* class recently identified by Soszyński et al. (2016). Other members of the class were identified in the Galactic bulge, M3, and Magellanic Clouds (Smolec et al. 2015; Jurcsik et al. 2014; Soszyński et al. 2016, respectively). *V3* and *V34* fit well within the region occupied by these stars in the Petersen diagram. Anomalous nature of the two RRd stars is discussed in more detail in Section 4.2.

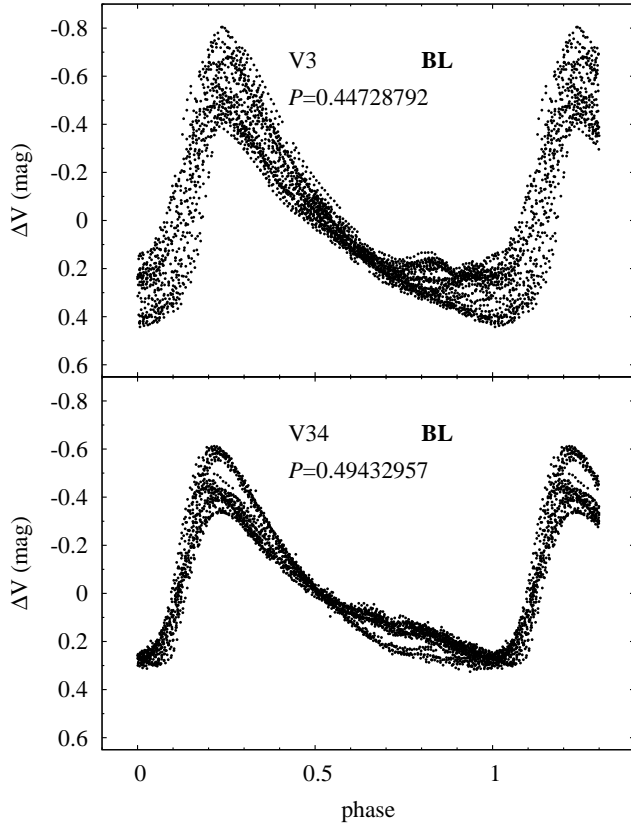
Periods and amplitudes of the two radial modes are given in Tab. 4. In both cases, first overtone amplitude constitutes only a small fraction of the fundamental mode amplitude, 7.3 and 5.7 per cent, for *V3* and *V34*, respectively. As already mentioned, the fundamental mode is strongly modulated in both stars. Properties of the modulation, determined from the analysis of the frequency spectrum, are summarized in Tab. 5. Modulation periods, ≈ 310 d and ≈ 784 d for *V3* and *V34*, respectively, are significantly longer than those in RRab or RRc stars. In both stars, modulation side peaks at the fundamental mode frequency have higher amplitude than the first overtone mode. Relative modulation amplitudes of the fundamental mode are ≈ 24 and ≈ 14 per cent for *V3* and *V34*, respectively. In *V3* a close peak is also detected in the vicinity of ν_1 , indicating a possible modulation of the first overtone with a period of ≈ 328 d, which is slightly different from the modulation period of the fundamental mode pulsation in the same star (≈ 310 d; see Tab. 5). The relative modulation amplitude for the first overtone mode is large, ≈ 43 per cent.

Table 4. Properties of the two analysed RRd variables: star’s id, fundamental mode and first overtone periods, period ratio, pulsation amplitudes of the fundamental and first overtone modes. Remarks: ‘BL’ – modulation of the radial mode(s) detected.

id	P_0 (d)	P_1 (d)	P_1/P_0	A_0 (mag)	A_1 (mag)	remarks
V3	0.44728792	0.3266817	0.7304	0.3771	0.0275	BL
V34	0.49432939	0.3596333	0.7275	0.3089	0.0177	BL

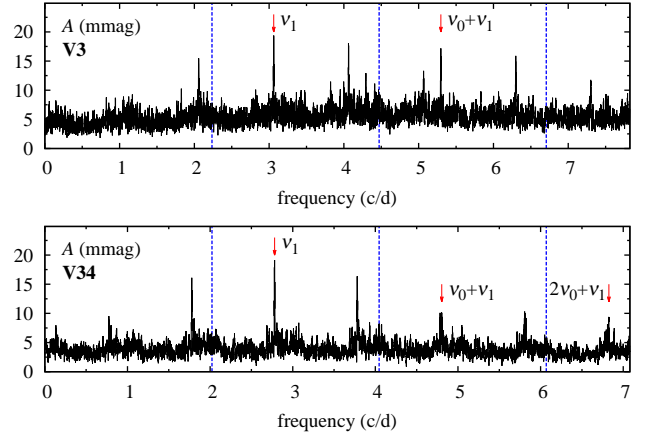
Table 5. Modulation properties of the anomalous RRd stars. Columns are the same as in Tab. 2 except the second column, which now identifies the pulsation mode. For each star, two rows are present: the first row refers to the modulation of the fundamental mode, the second row to the modulation of the first overtone.

star id	mode	P (d)	P_m (d)	A_- (mag)	A_+ (mag)	A_{mod}	Q	data	main modulation components
V3	F	0.44728792	310.07	0.0365	0.0913	0.242	0.429	all	$\pm\nu_{m1}$ components at $\nu_0, \dots, 4\nu_0$; $+\nu_{m1}$ components at $5\nu_0, \dots, 7\nu_0$
	1O	0.3266817	327.8	–	0.0117	0.425	1.000		$+\nu_{m2}$ component at ν_1
V34	F	0.49432939	784.3	–	0.0421	0.136	1.000	all	$+\nu_m$ components at $\nu_0, \dots, 7\nu_0$
	1O	0.3596333	no modulation detected						

**Figure 10.** Light curves of the two RRd variables phased with the fundamental mode period. In both cases the first overtone is of a low amplitude, and scatter present in both light curves is mostly due to Blazhko modulation.

3.7 The case of V37

V37 was identified by O01 as RR Lyr star pulsating in the first overtone. Its location in the period-amplitude diagram (Fig. 2) and colour-magnitude diagram (Fig. 3) is extreme, but based on these diagrams only, the star could be regarded as hot, short-period RRc star of low pulsation amplitude

**Figure 11.** Detection of the first overtone in V3 (top) and V34 (bottom). The plots show the frequency spectrum for the two stars after prewhitening with the fundamental mode frequency, its harmonics (dashed lines) and all detected modulation peaks located close to $k\nu_0$. The pronounced signal from the first overtone is marked with an arrow. Several combination frequencies are detected and also marked.

(likely located at the blue edge of the instability strip). Its pulsation properties indicate it is not the case, however. Its phased light curve, presented in the top panel of Fig. 12, shows that the star is multiperiodic or modulated. Indeed, the frequency spectrum of V37 is rich; three independent periodicities are identified. Tab. 6 provides frequencies, amplitudes and phases of all significant peaks identified in the frequency spectrum. The last two columns provide two possible interpretations. In both of them, the frequency of the highest amplitude peak is denoted by ν_1 ; it corresponds to the dominant period identified as due to radial first overtone in O01. The second highest peak in the spectrum is located very close to ν_1 (its frequency is higher by ≈ 0.0634 c/d) and can be interpreted twofold. In the first scenario (‘modulation?’; fourth column of Tab. 6), it is due to a modulation of the dominant variability. The separation between the two dominant peaks corresponds to the modulation fre-

quency and is denoted by ν_{m1} . Other significant peaks in the frequency spectrum are components of the modulation multiplet, as given in the fourth column of Tab. 6. In the second scenario (‘beating?’; fifth column of Tab. 6), the second highest peak in the spectrum is treated as an independent frequency, denoted by ν_x . Other peaks in the spectrum are then its harmonics or linear combination frequencies with ν_1 . In addition to the two dominant frequencies and their linear combinations, we also detect an equidistant triplet centered on ν_1 (peaks at $\nu_1 - \nu_{m2}$ and at $\nu_1 + \nu_{m2}$), which, in both scenarios, is attributed to modulation of ν_1 with the period of ≈ 58.4 d and with a rather low relative modulation amplitude, of 5.7 per cent. In the first scenario, we have one dominant variability modulated with two periods. In the second scenario, we deal with a double-periodic variability, with a weak modulation of the dominant periodicity. Which of the two scenarios is more plausible?

A glimpse at the fourth column of Tab. 6 points, that the modulation scenario is unrealistic. Highly incomplete, high-order multiplets are detected in the spectrum: quintuplet at $2\nu_1$, septuplet at $3\nu_1$ and nonuplet at $4\nu_1$. Only the highest frequency component of the nonuplet is detected in the vicinity of $4\nu_1$ and only two highest frequency components of the septuplet are detected in the vicinity of $3\nu_1$. The harmonics themselves, $3\nu_1$ and $4\nu_1$, are not detected at all. Such a picture of modulation is unrealistic, needles to say it was not detected in any variable so far. At the same time, the beating scenario (fifth column of Tab. 6) provides a simple and realistic alternative explanation. Two close, highest amplitude peaks in the frequency spectrum are interpreted as two independent periodicities. One harmonic of ν_1 and three harmonics of ν_x are detected, as well as several low-order combination frequencies which are expected for double-periodic variability. In addition, the dominant variability is modulated, as the equidistant triplet centred on ν_1 indicates. Period ratio, $P_x/P_1 = 0.9841$, indicates that the two periodicities cannot correspond to two radial modes; at least one must correspond to a non-radial pulsation or its origin is not due to pulsation at all. The two periodicities can be easily separated and the resulting light curves are presented in the middle and bottom panels of Fig. 12. Interestingly, it is the lower amplitude light curve that is more non-sinusoidal, whereas the light curve corresponding to the higher amplitude variability is nearly symmetric. In both cases the corresponding Fourier parameters are not typical for RRc variability – see Fig. 13. In particular, Fourier phase, φ_{21} , is significantly lower than expected for RRc stars of similar period. Light curve shape, position in the period-amplitude and colour-magnitude diagrams and presence of two close, high-amplitude periodicities – altogether rule out the possibility that V37 is an RRc star. What kind of variable is it, then?

The characteristic shape of the light curve plotted in the bottom panel of Fig. 12 (P_x) suggests, it is due to pulsation, most likely in the radial fundamental mode. In fact, the light curve shape and the corresponding Fourier decomposition parameters are typical for high amplitude δ Scuti stars (HADS; see eg. Poretti 2001). These stars often pulsate in two radial modes, fundamental and first overtone. The longest period of the fundamental mode in these double mode variables is ≈ 0.22 d (Poretti et al. 2005), but in other HADS it can reach up to ≈ 0.3 d. The period of V37 is

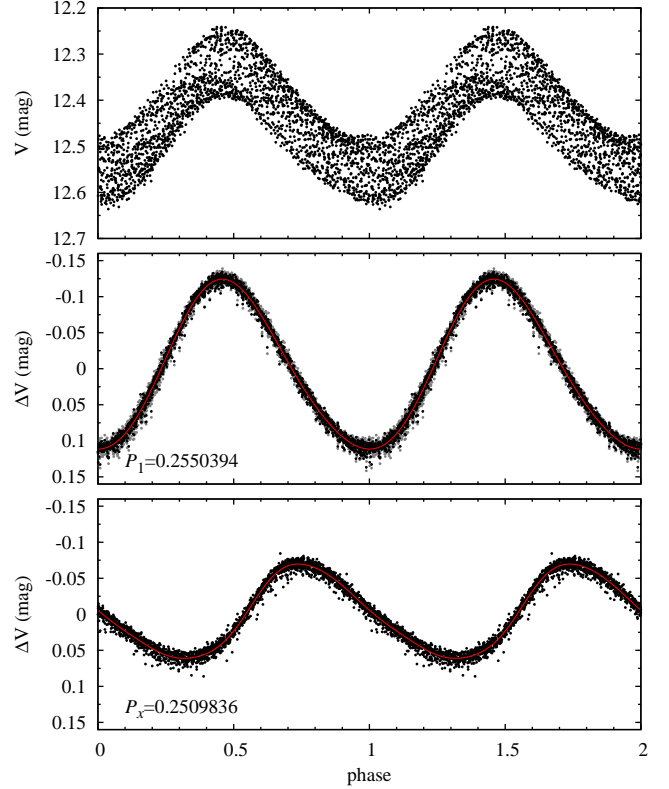


Figure 12. Top panel: light curve of V37 phased with $P_1 = 0.2550394$ d. The large scatter is mostly due to beating of two periods, P_1 , and a bit shorter period, $P_x = 0.2509836$ d. Disentangled light curves corresponding to these two periodicities are plotted in the middle (P_1) and in the bottom (P_x) panels, with second and fourth order Fourier fits over-plotted (red solid line).

a bit longer than 0.22 d, and it pulsates in one radial mode at most. However, genuine δ Sct stars are not expected to be observed in NGC 6362, as the turn off mass in the cluster is around 0.8 solar masses (Kaluzny et al. 2015). V37 could be a merger, just as it is suspected for SX Phe stars, six of which are detected in NGC 6362 (Kaluzny et al. 2014). Light curves of SX Phe stars can be similar to that of V37, but their periods are much shorter and they are by ≈ 2 mag fainter (Mazur et al. 1999; Kaluzny et al. 2014).

The presence of the additional periodicity does not provide much help; in fact its origin is even more puzzling. A non-radial mode of a much higher amplitude and only slightly non-sinusoidal light curve seems not probable. Slight asymmetry and short period, $P_1 \approx 0.255$ d, seem to rule out the possibility that this variability is due to rotation or binarity effects. We stress that both periodicities are intrinsic to V37 as we detect several strong combination frequencies, which are also prominent in the flux data. Combination frequencies in the flux data, in principle may also result from a non-linearity of the CCD detector. However, two combination frequencies are detected also in the data gathered with the du Pont telescope (these data are less numerous and of inferior quality, though). Hence, we conclude that the two dominant periodicities observed in V37 must be both intrinsic to this variable. The puzzling frequency spectrum of V37 does not result from blending of two stars.

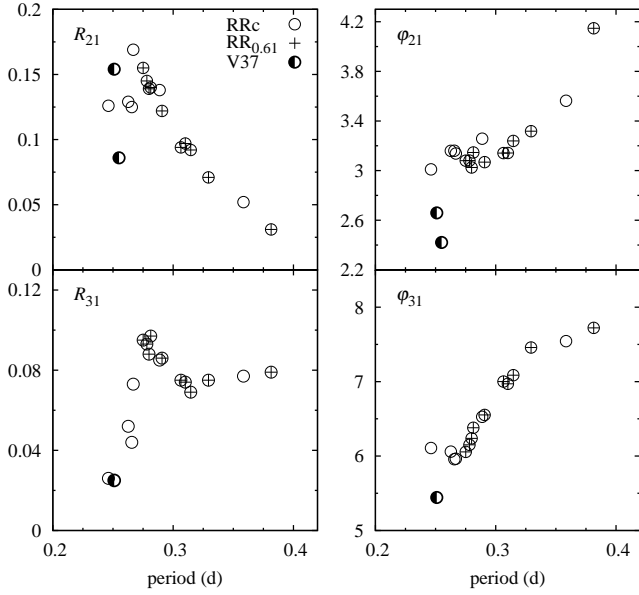


Figure 13. Low-order Fourier decomposition parameters for RRc stars and for the peculiar variable V37 (half-filled symbols). For V37 two points are plotted for R_{21}/φ_{21} which correspond to two dominant periodicities detected in this star.

The possibility that V37 is not a genuine member of NGC 6362 would allow more speculations. We note however, that [Zloczewski et al. \(2012\)](#) lists V37 among genuine proper motion members of the cluster. Hence, location of V37 in the colour-magnitude diagram, in particular, its mean brightness, typical for horizontal branch stars, is important constraint for any explanation of its nature. Such explanation is clearly lacking at the moment. We note that just recently, we have discovered a very similar variable among RRc stars in the OGLE Galactic bulge collection ([Netzel & Smolec, in prep.](#)). Its properties are also best explained as beating of two very close periodicities. The light curve shapes are very similar to that displayed in [Fig. 12](#) for V37. Hence, V37 might not be an isolated, peculiar case, but may represent a new type of variability.

4 DISCUSSION

4.1 Blazhko effect in NGC 6362

The incidence rate of the Blazhko phenomenon in NGC 6362, 69 per cent for RRab stars and 19 per cent for RRc stars, is very high – among the highest reported in ground-based observations published so far. We note however that studies of the Blazhko modulation in globular clusters, based on top-quality observations and Fourier analysis (which is essential for firm confirmation of the Blazhko effect⁴) are scarce. For M3, [Jurcsik & Smitola \(2016\)](#) reports

⁴ Some studies classify RR Lyr stars as Blazhko, based on the appearance of the light curve only – its scatter or non-repeating shape (e.g. [Arellano Ferro et al. 2012](#); [Kunder et al. 2013](#)). With such an approach, the presence of a quasi-periodic modulation cannot be firmly established. As a result, spurious, exceedingly high incidence rates are sometimes reported.

Table 6. Two interpretations for V37. The first three columns list frequencies, amplitudes and phases of significant peaks detected in the frequency spectrum of V37. The following two columns provide two possible interpretations: ‘modulation’ and ‘beating’ scenarios.

ν (c/d)	A (mag)	ϕ (rad)	modulation?	beating?
0.06336058	0.0053	5.82	ν_{m1}	$\nu_x - \nu_1$
3.90384907	0.0067	5.18	$\nu_1 - \nu_{m2}$	$\nu_1 - \nu_{m2}$
3.92096263	0.1169	1.73	ν_1	ν_1
3.93807620	0.0029	2.31	$\nu_1 + \nu_{m2}$	$\nu_1 + \nu_{m2}$
3.98432322	0.0645	6.09	$\nu_1 + \nu_{m1}$	ν_x
4.04768380	0.0059	0.30	$\nu_1 + 2\nu_{m1}$	$2\nu_x - \nu_1$
7.84192527	0.0101	5.88	$2\nu_1$	$2\nu_1$
7.90528585	0.0070	3.60	$2\nu_1 + \nu_{m1}$	$\nu_x + \nu_1$
7.96864643	0.0099	2.26	$2\nu_1 + 2\nu_{m1}$	$2\nu_x$
11.88960907	0.0043	5.71	$3\nu_1 + 2\nu_{m1}$	$2\nu_x + \nu_1$
11.95296965	0.0017	4.86	$3\nu_1 + 3\nu_{m1}$	$3\nu_x$
15.93729287	0.0012	1.33	$4\nu_1 + 4\nu_{m1}$	$4\nu_x$

47 and 11 per cent incidence rates for RRab and RRc stars, respectively. In M5, 36 per cent of RRab stars show the Blazhko modulation ([Jurcsik et al. 2011](#)). For the field, the top-quality ground-based observations and space observations show, that the incidence rate among RRab stars is close to 50 per cent (e.g. [Jurcsik et al. 2009](#); [Kovács 2016](#)).

We stress that the reported high incidence rate of the Blazhko phenomenon results not only from the top quality of the data we analyse and consequently the low detection threshold in the mmag range. In fact, modulation is easily detected because of large modulation amplitudes. The amplitude of the dominant modulation side peak in the vicinity of the radial mode frequency is at least 3.5 mmag for RRc stars and at least 9 mmag for RRab stars. Although the detection of 3.5 mmag signals is indeed challenging in typical ground based data, identifying signals at the level of 9 mmag is rather routine in the data of massive sky surveys (see e.g. analysis of OGLE-III data by [Netzel, Smolec & Moskalik 2015a](#)). The relative modulation amplitudes for RRab stars range from 3 to 24 per cent and for RRc stars from 2 to 28 per cent.

All modulation periods are below 100 d with the exception of the second modulation period detected in V30, which is ≈ 216.4 d. V30 is the only RRab star in which two modulation periods were detected. Two modulation periods were also detected in RRc variable, V6, but the secondary modulation is very weak. [Benkó et al. \(2014\)](#) noted, based on the analysis of the *Kepler* sample, that the ratio between the primary and secondary modulation periods is nearly always close to a small integer number. We note that the two modulation periods in V30 and V6 are not in a resonant or close-to-resonant ratio as P_{m1}/P_{m2} is ≈ 0.16 for V30 and ≈ 1.12 for V6.

In the colour-magnitude diagram ([Fig. 3](#)) we marked the Blazhko variables with thick symbols. Two of the three modulated RRc stars, V6 and V10, are among the hottest RRc stars of NGC 6362. V36 on the other hand, in which the Blazhko modulation is weak (only one modulation side peak was detected), is the coolest RRc star in the sample. The majority of RRab stars show the Blazhko effect; they are scattered over the entire domain of RRab stars in the diagram.

The only two RRd variables we identified in NGC 6362 show modulation of the radial modes, which is characteristic for anomalous RRd stars. Incidence rate of the Blazhko effect among M3 double-mode variables is 45 per cent; 4 modulated RRd stars of M3 also have anomalous period ratios (Jurcsik et al. 2014; Jurcsik & Smitola 2016); see next section for more details.

Finally, we note that in some of the Blazhko variables, the phase coverage of the modulation cycle is very good, and the Blazhko effect itself appears regular. It allows to visualise the light curve changes over the Blazhko cycle in the form of an animation. Such animations for V5, V31 (RRab) and V10 (RRc) are available as a supplementary on-line material. Data for these stars were phased with the modulation period, divided into ten phase bins, and phased with the pulsation period within each bin. Fig. 14 illustrates the light curve changes in V10. Both amplitude and phase modulation are apparent. At phases of lower pulsation amplitude ($\phi_B = 0.6, \dots, 0.9$) the light curve is essentially featureless. As pulsation amplitude gets higher, the shoulder (or bump) appears on the ascending branch, just before the maximum brightness.

4.2 Anomalous RRd stars in NGC 6362

Recently, the new class of multiperiodic RR Lyr pulsators was identified: anomalous RRd stars (Soszyński et al. 2016). In these variables, two radial modes, fundamental and first overtone, are involved in the pulsation, but otherwise properties of these stars are anomalous, as compared to “classical” RRd stars. The first objects of this type were discovered in the Galactic bulge (Soszyński et al. 2014; Smolec et al. 2015) and in the globular cluster M3 (Jurcsik et al. 2014). Only recently additional objects were detected in the OGLE Magellanic Clouds photometry by Soszyński et al. (2016), who proposed to call these stars anomalous RRd, based on their distinct characteristics. Location of these stars in the Petersen diagram does not follow the well defined progression delineated by “classical” RRd stars; their period ratios are significantly different than in the classical RRd stars at the same fundamental mode period. Typically, the period ratios are smaller. This is well illustrated in Fig. 15. Contrary to “classical” RRd stars it is the fundamental mode that most often dominates the pulsation. Finally, a long-term modulation of pulsation of one, or of both radial modes is often detected in anomalous RRd stars. Soszyński et al. (2016) also noted a somewhat peculiar light curve shape of the dominant fundamental mode variation.

The two RRd stars newly detected in NGC 6362, V3 and V34, clearly belong the class of anomalous RRd stars, as they share the same characteristics. Their period ratios are lower than expected at a given fundamental mode period. In both stars it is the fundamental mode that dominates the pulsation. Finally, a modulation of the radial modes is firmly detected in both V3 and V34.

It is important to note that anomalous RRd stars are not a homogeneous group. Although all reported stars share the same broad characteristics (e.g. anomalous period ratios, modulation), some systematic differences can be easily pointed out while analysing stars of different stellar systems. Contrary to classical RRd stars, the fundamental mode usually has a larger amplitude than the first overtone. In the

Magellanic Clouds it is the case for 19 out of 22 stars, which is 86 per cent of the sample (see tab. 1 in Soszyński et al. 2016). In M3, in three out of four anomalous RRd stars the fundamental mode dominates (75 per cent; Jurcsik et al. 2014). Interestingly, the only star in which the first overtone dominates the pulsation (V99) has a higher period ratio than the classical RRd stars. In the Galactic bulge, only in 7 out of 15 stars reported by Smolec et al. (2015) the fundamental mode dominates, which constitutes 47 per cent of the sample. Still, this number is higher than in the population of classical RRd stars in the same stellar system, where it is only 18 per cent. Further, if we exclude a few stars with larger period ratios, in 70 per cent of anomalous RRd stars of the Galactic bulge the fundamental mode dominates. In the only two anomalous RRd stars of NGC 6362, the fundamental mode strongly dominates. In fact, the amplitude ratios, 7.3 and 6.6 per cent in V3 and V34, respectively, are the smallest reported for anomalous RRd stars.

Further differences are noticed in the modulation properties of RRd stars with anomalous period ratios, most notably in the asymmetry of modulation side peaks. In the modulated stars of the Magellanic Clouds in all but one star, the modulation side peaks on the lower frequency side of the radial mode are higher (see tab. 2 in Soszyński et al. 2016). Relevant information is also available for the Galactic bulge stars, in which there is no clear tendency: side peaks on either side of the radial mode frequency can be higher (see tab. 2 in Smolec et al. 2015). In the two RRd stars of NGC 6362 the modulation side peaks on higher frequency side of the radial mode dominate or are the only side peaks detected.

A study of systematic differences between anomalous RRd stars of different stellar systems is important for testing the models explaining the origin of this peculiar form of pulsation. So far, only one mechanism was proposed. Based on linear pulsation models, Soszyński et al. (2016) pointed out that anomalous RRd pulsation might be related to the parametric resonance of the form: $2\nu_1 = \nu_0 + \nu_2$. In this scenario, a low damping rate of the fundamental mode is needed to explain its typically higher amplitude, as fundamental mode is a *daughter mode*, gaining energy at the cost of the first overtone. A modulation of pulsation amplitude and phase is also, in principle, possible in this resonance scenario. Nevertheless, to validate the proposed mechanism, and to provide any predictions that could be compared with observations, non-linear model computations are needed.

4.3 Non-radial pulsation in RRc stars

Earlier detections. Detection of non-radial modes was claimed in the observations of globular cluster M55 (Olech et al. 1999), and in NGC 6362 (O01). O01 lists three stars as showing non-radial pulsations: V6, V10 and V37. V37 is very peculiar object and we discussed it in detail in Section 3.7. Now we focus on V6 and V10. The suspected non-radial modes were identified by O01 based on the frequency spectrum analysis, as peaks close to the radial mode frequency. In V6 and V10 two close peaks, symmetrically placed around the radial mode frequency, were detected. Such peaks, forming equidistant triplet with the radial mode frequency, might also appear as due to modulation of pulsation, i.e. the Blazhko effect. For these stars, the correspond-

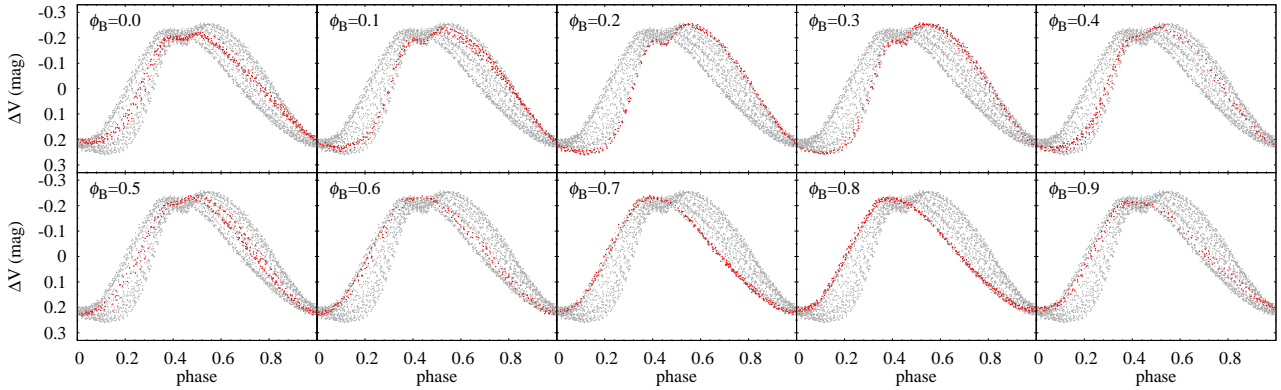


Figure 14. Illustration of the Blazhko effect in RRc variable V10; snapshots from the animation available as supplementary on-line material.

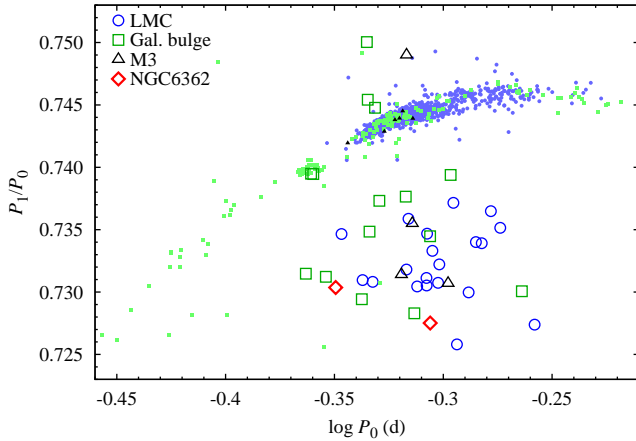


Figure 15. Petersen diagram for classical and anomalous RRd stars of various stellar systems: Galactic bulge (green squares), LMC (blue circles), M3 (black triangles) and NGC 6362 (red diamonds). Classical and anomalous RRd stars are plotted with small filled symbols and with large open symbols, respectively.

ing modulation periods would be 15.5 d and 8.5 d, for V6 and V10, respectively. Because at that time the known Blazhko RRc stars were scarce and all Blazhko RRc stars reported in the literature had longer modulation periods, O01 interpreted the additional periodicities as due to non-radial pulsation. We also note that some of the early models do explain the Blazhko effect as a beating between the radial mode and non-radial, $\ell = 1$ modes, excited by the 1:1 resonance with the radial mode. The non-radial modes are split due to star's rotation and form a symmetric triplet with the radial mode frequency (Nowakowski & Dziembowski 2001). The better and better photometric data gathered over the past several years seem to falsify such a model, though (for recent reviews, see eg., Kovács 2016; Smolec 2016). In many stars the modulation is clearly not regular, consecutive modulation cycles, their length and shape, differ. In several stars, including the ones reported here, double-periodic modulation was detected. These observations cannot be explained by clock-work models, like that of Nowakowski & Dziembowski (2001). In addition, the close peaks seen in the frequency spectrum appear to be parts of multiplet structures which are a signature of genuine modulation. Due to the poor qual-

ity of the observations only one or two components of the multiplet were detected in the past. Several examples can be given for NGC 6362. When results of O01 and of the present analysis are compared, we commonly detect triplets (V7, V18, V30, V31, V32), full quintuplets or components of quintuplet structure (V1, V5, V29, V6, V10) or even septuplet components (V13) in place of a single close peak detected in the earlier study of O01. This concerns both RRab and RRc stars. In particular, for V6 and V10 we find full quintuplet around at least one harmonic of ν_1 , see the last column of Tab. 2. These stars are classified as genuine Blazhko RRc variables in our study. We also note that several RRc stars with an even shorter modulation periods are now known (see e.g. Skarka 2013).

Variability in the $(0.60, 0.65)P_1$ range. Starting with AQ Leo observed with the space telescope *MOST* (Gruberbauer et al. 2007), in many RRc and RRd stars additional signals in the $P_x/P_1 \in (0.60, 0.65)$ range and with amplitudes at the mmag level were reported ($\nu_{0.61}$ peaks; e.g. Olech & Moskalik 2009; Netzel, Smolec & Moskalik 2015a,b). This is particularly true for the space observations, as nearly all RRc and RRd stars observed from space show this form of pulsation (e.g. Szabó et al. 2014; Moskalik et al. 2015; Molnár et al. 2015). Consequently, $\nu_{0.61}$ frequencies must be common in the RRc/RRd variables, but it is challenging to detect them from the ground, because of a higher noise in the ground-based photometric data. In the Petersen diagram, the stars group in three sequences: in the most populated, bottom sequence, centred at $P_x/P_1 \approx 0.613$, in the middle, least populated sequence, centred at 0.623, and in the top sequence centred at 0.631 (see Fig. 16). The middle sequence was first recognized after analysis of the top-quality sample of RRc stars observed by the OGLE project (Netzel, Smolec & Moskalik 2015b). In fact, most of the known RR_{0.61} stars were discovered in the OGLE Galactic bulge data and these stars are marked in Fig. 16 separately, with small bluish squares. The above quoted average period ratios are from Netzel, Smolec & Moskalik (2015b) and are based on the OGLE Galactic bulge data only. In Fig. 16 we also included M3 sample from Jurcsik et al. (2015) (black diamonds), ω Cen sample from Olech & Moskalik (2009) (green triangles) and all other known stars of this type, mostly from space observations (red open squares). In several stars, subharmonics of the additional frequencies, i.e.

peaks centred at $\frac{1}{2}\nu_{0.61}$ and $\frac{3}{2}\nu_{0.61}$ were reported (see eg., Moskalik et al. 2015; Molnár et al. 2015; Kurtz et al. 2016). In the frequency spectrum, the $\nu_{0.61}$ peaks and peaks at the subharmonic frequencies are often non-coherent and appear as a clump of peaks or as a wide power excesses.

The model of Dziembowski (2016) explains the $\frac{1}{2}\nu_{0.61}$ subharmonics as due to non-radial strongly-trapped modes of $\ell = 8$ (for the top sequence in the Petersen diagram) and $\ell = 9$ (for the bottom sequence). Such modes have low observed amplitudes because of a strong geometric cancellation and are rarely detected in RR_{0.61} stars. On the other hand, harmonics of these non-radial modes should have higher observed amplitudes because of only weak geometric cancellation and because of non-linear effects. These harmonics correspond to the $\nu_{0.61}$ periodicities commonly observed in RRc and RRd variables. The middle sequence in the Petersen diagram of RR_{0.61} stars is explained by a combination frequency, $\nu_8 + \nu_9$. In this scenario, $\nu_{0.61}$ peaks are in fact multiplets, which, due to nonlinear mode interaction, have a complex form in the frequency spectrum.

We note that $\nu_{0.61}$ peaks are also detected in the first overtone Cepheids (e.g. Moskalik & Kołaczowski 2009; Soszyński et al. 2010). The distribution of period ratios of stars showing the $\nu_{0.61}$ peaks with and without subharmonics, both in Cepheids and in RR Lyr stars, strongly supports Dziembowski’s model (Smolec & Śniegowska 2016).

We do not detect subharmonics in RR_{0.61} stars of NGC 6362. In one star, V17, we detect periodicities that correspond to the three sequences in the Petersen diagram (see Tab. 3 and Fig. 8). The ‘middle periodicity’ should correspond to the combination frequency then. In Fig. 8, we indicate where the combination frequency is expected (arrow marked with ‘c’ label), based on the frequencies of the highest peaks corresponding to the bottom and top sequences (marked with left-most and right-most arrows in the same panel; $2\nu_8$ and $2\nu_9$ according to the Dziembowski’s model). It indeed falls very close to the location of the highest peak corresponding to the middle sequence in the Petersen diagram. Although the agreement is not perfect, it is satisfactory, taking into account the complex appearance of the $\nu_{0.61}$ peaks and consequently, intrinsic difficulty in precise determination of their frequency. We note that all other known RRc/RRd stars with periodicities corresponding to the three sequences in the Petersen diagram pass this test (Dziembowski & Smolec, in prep.).

Properties of RR_{0.61} stars in the globular clusters. A large fraction of RRc stars in the globular cluster M3, 38 per cent (14 out of 37 RRc), are RR_{0.61} stars. In addition, in 4 out of 10 RRd stars (40 per cent) $\nu_{0.61}$ peaks were detected (Jurcsik et al. 2015). One of these RRd stars is anomalous. The incidence rate is even higher among RRc stars of NGC 6362 as in 10 out of 16 RRc stars (63 per cent) we detect $\nu_{0.61}$ peaks. It is the highest incidence rate in the published ground-based observations. In the Petersen diagram, Fig. 16, NGC 6362 variables nicely fit the three sequences formed by the previously discovered objects, majority of which are Galactic bulge stars. The only exception is V8 for which period ratio is low, 0.6080 (Tab. 3); still a few objects with similar period ratios were reported in the literature and are included in Fig. 16. In all but two stars we detect only a single additional periodicity that falls within the bottom sequence in the Petersen diagram.

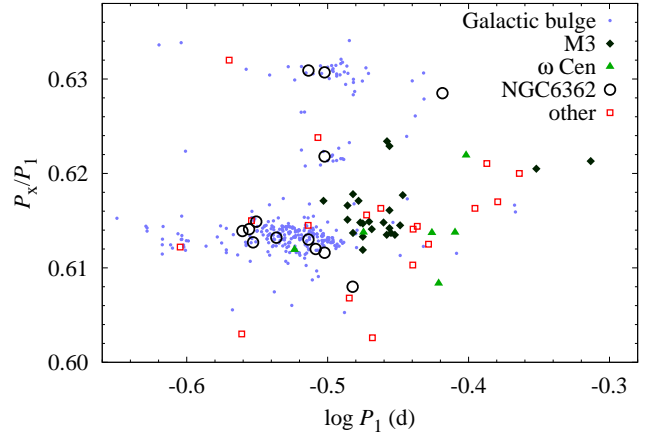


Figure 16. Petersen diagram for RRc stars with additional variability in the $P_x/P_1 \in (0.60, 0.65)$ range.

In V33 two additional periodicities are detected, and they correspond to the bottom and to the top sequence in the Petersen diagram. In V17 three periodicities are detected that nicely fit to the three sequences delineated by the OGLE Galactic bulge stars. A systematic difference with M3 stars is apparent. First, RR_{0.61} stars of M3 are shifted towards longer periods. The shift is consistent with the difference of average RRc periods in both clusters, which is $\langle P_{RRc} \rangle_{M3} - \langle P_{RRc} \rangle_{NGC6362} \approx 0.042$ d. The scatter among RR_{0.61} stars of M3 seems larger; their mean period ratio is also slightly higher than that derived from the Galactic bulge sample. In fact, the Galactic bulge RR_{0.61} stars are scarce at first overtone periods characteristic for M3 RR_{0.61} stars. Only six RR_{0.61} stars were identified in ω Cen (Olech & Moskalik 2009). Four of them have first overtone periods longer than typically observed for RR_{0.61} stars of M3 and of NGC 6362. Two have shorter periods, one within the range typical for M3 stars, and the other within a range typical for NGC 6362 stars. In general, RR_{0.61} stars of ω Cen are strongly scattered over the Petersen diagram.

The described differences in the distribution of RR_{0.61} stars of the three globular clusters in the Petersen diagram must reflect the metallicity and population differences between the three clusters. Both M3 and NGC 6362 are OoI, but their mean metallicities differ, $[Fe/H] = -1.57$ and $[Fe/H] = -0.95$, for M3 and NGC 6362, respectively. Also, M3 has been assigned to a young, while NGC 6362 to an old halo population (Mackey & van den Bergh 2005) (although the isochrone fitting yields the same age for both systems Dotter et al. 2010). The metallicity difference alone cannot explain the observed period shift between RR_{0.61} stars of the two clusters. ω Cen, on the other hand, is a very large and atypical globular cluster. It is classified as OoII type and its mean metallicity ($[Fe/H] = -1.62$) is similar to M3, but it is known to host diverse stellar populations and might be a remnant of the dwarf galaxy (e.g., Catelan 2009). It explains why its RR_{0.61} stars are scattered over the Petersen diagram; long periods of its four RR_{0.61} stars are consistent with its OoII designation.

Based on their analysis, Jurcsik et al. (2015) pointed out two interesting properties of RR_{0.61} variables, which we can check for NGC 6362 stars. First, they noted, the

RR_{0.61} stars are located in the colour-magnitude diagram (see their fig. 3) in the region directly adjacent to the RRd domain (to its blue side; we note that $\nu_{0.61}$ peaks were also detected in RRd stars in their study). In the colour magnitude-diagram plotted in our Fig. 3, we marked the RR_{0.61} stars with the plus sign. It is hard to define the RRd domain in this plot, as we have only two anomalous RRd stars in our sample. However, the interface between RRab and RRc stars is clearly marked. No doubt, the RR_{0.61} stars concentrate on the blue side of this interface. We thus confirm the observation made by Jurcsik et al. (2015). Second, analysing the light curves and corresponding Fourier decomposition parameters for RRc stars with and without $\nu_{0.61}$ peaks, Jurcsik et al. (2015) concluded (see their fig. 4), that light curves of RR_{0.61} stars are “sinusoidal, with a reduced, if any, bump preceding maximum brightness”. In Fig. 13 we plot the low-order Fourier decomposition parameters for RRc stars and mark the RR_{0.61} stars with plus sign. Contrary to Jurcsik et al. (2015), we observe that there is no difference between R_{21} and R_{31} of RR_{0.61} stars and other RRc stars. Also, a glimpse at Fig. 6 indicates that the bump preceding maximum brightness is commonly present in RR_{0.61} stars of NGC 6362 (e.g. in V23, V27, V15, V21). We conclude that there is no specific feature of the light curve that distinguishes the RR_{0.61} phenomenon in general.

We do not detect subharmonics in RR_{0.61} stars of NGC 6362. Subharmonics were not detected in M3 either. Jurcsik et al. (2015) detected $\nu_{0.61}$ peaks in 4 RRd variables, including one anomalous star. We find no trace of $\nu_{0.61}$ peaks in the only two, anomalous RRd stars of NGC 6362.

Gravity modes in RRc stars? In two RRc variables we have detected additional long-period variability; too slow to be associated with an acoustic mode of oscillation. On the other hand, additional periods are too short to be connected with rotation or with binarity effects. If these periodicities are intrinsic to the stars, they would correspond to non-radial, gravity mode pulsation. Detection of long-period additional variability in the RRc stars was also reported in the analysis of top-quality *Kepler* observations, see section 6 in Moskalik et al. (2015). We stress that possible detection of gravity modes in giant-type stars represents a challenge to stellar pulsation theory (Dziembowski 1977).

In the case of V8 and V35 (see Section 3.5) the additional variability is in the mmag regime. In no case we have detected combination frequencies with the dominant radial oscillation, so we have no proof that additional periodicities are intrinsic to these stars. Contamination is likely in the dense fields of globular cluster. Consequently, we refrain from any definite statements on the nature of additional long-period variabilities in the discussed stars.

5 SUMMARY AND CONCLUSIONS

We have analysed top-quality photometric data gathered for 35 RR Lyr stars in the globular cluster NGC 6362 within the CASE project. Our most important findings are the following.

- Sixteen of the analysed stars are genuine RRab stars and other 16 are genuine RRc stars, in agreement with earlier studies of RR Lyr stars in NGC 6362.

- Two stars previously classified as RRab, V3 and V34, are anomalous RRd stars, members of the recently identified class of double-mode pulsators. In addition to the radial fundamental mode we detect the radial first overtone of low amplitude. Period ratio of the two radial modes is significantly lower than for the majority of ‘classical’ RRd stars at the same fundamental mode period. In both stars, either both radial modes are modulated (V3), or only one of the modes is modulated. Previously, anomalous RRd stars were identified in the Galactic bulge, the Magellanic Clouds and in the globular cluster M3.

- V37, previously classified as RRc, shows beating of two close and large amplitude periodicities. The presence of combination frequencies in the flux data confirms that both are intrinsic to the star. Surprisingly, lower amplitude periodicity is more nonlinear; its characteristic shape, with short ascending branch and long descending branch, suggest that it is due to pulsation in the radial fundamental mode. The light curve corresponding to the dominant variability is more symmetric; a weak modulation of this signal was also detected. Both light curves significantly differ from the shape typical for RRc stars. Its RR Lyr classification is thus tentative; however, we cannot propose other satisfactory explanation of its nature. We note that the star is a genuine proper-motion member of the cluster and its brightness is typical for horizontal branch stars in NGC 6362.

- Ten out of 16 RRc stars show additional periodicities in the $(0.60, 0.65)P_1$ range. These double-periodic variables, abbreviated here as RR_{0.61}, are well known; in fact, based on space observations, it is expected that this form of pulsation must be common among RRc/RRd stars. The incidence rate in NGC 6362, 63 per cent, is the highest in ground-based observations published so far. Properties of RR_{0.61} stars in NGC 6362 are qualitatively similar to properties of RR_{0.61} stars in the Galactic bulge; in particular their location in the Petersen diagram is very similar. RR_{0.61} stars of NGC 6362 fall within the three sequences formed by the Galactic bulge stars. Systematic differences are noted when RR_{0.61} stars of NGC 6362 are compared with RR_{0.61} stars of other globular clusters, M3 and ω Centauri. Numerous populations of RR_{0.61} stars in different stellar systems are essential for testing the models which try to explain the nature of RR_{0.61} stars.

- Our results support the observation made by Jurcsik et al. (2015) in M3: RR_{0.61} stars tend to cluster on the cool side of the RRc domain, at the interface with RRab domain, where RRd pulsation is also expected.

- Incidence rate of the Blazhko effect is among the highest reported in the ground-based observations. We detect modulation in 11 out of 16 RRab stars (69 per cent) and in 3 out of 16 RRc stars (19 per cent). In addition, one RRc star and one RRab star are rare examples of stars in which two modulation periods are detected.

- RRc stars are prone to phase instabilities. These rarely correspond to steady period increase/decrease, but in the majority of cases have complex nonlinear appearance and occur on time scales much shorter than expected due to evolution. In contrast, majority of RRab stars have stable pulsation periods over the time span of the observations.

ACKNOWLEDGEMENTS

PM and RS were supported by the grants DEC-2012/05/B/ST9/03932 and DEC-2015/17/B/ST9/03421, and JK and WP were supported by the grant DEC-2012/05/B/ST9/03931 from the National Science Centre, Poland.

REFERENCES

- Alard C., Lupton R.H., 1998, *ApJ*, 503, 325
 Alcock C., et al., 2003, *ApJ*, 598, 597
 Arellano Ferro A., Bramich D.M., Figuera Jaimes R., Giridhar S., Kuppuswamy K., 2012, *MNRAS*, 420, 1333
 Benkő J.M. et al., 2014, *ApJS*, 213, 131
 Le Borgne J.F., et al., 2014, *MNRAS*, 441, 1435
 Bryant P.H., 2016, *ApJ*, 818, 53
 Buchler J.R., Kolláth Z., 2011, *ApJ*, 731, 24
 Catelan M., 2009, *Ap&SS*, 320, 261
 Dotter A., et al., 2010, *ApJ*, 708, 698
 Dziembowski W., 1977, *Acta Astron.*, 27, 95
 Dziembowski W., 2016, *Comm. Konkoly Obs.*, 105, 23
 Gruberbauer M. et al., 2007, *MNRAS*, 379, 1498
 Guggenberger E., et al., 2012, *MNRAS*, 424, 649
 Harris, W. E. 1996, *AJ*, 112, 1487
 Jurcsik J., Smitola P., 2016, *Comm. Konkoly Obs.*, 105, 167
 Jurcsik J., Szeidl B., Clement C., Hurta Zs., Lovas M., 2011, *MNRAS*, 411, 1763
 Jurcsik J., et al., 2009, *MNRAS*, 400, 1006
 Jurcsik J., et al., 2014, *ApJ* 797, L3
 Jurcsik J., et al., 2015, *ApJ Suppl. Ser.*, 219, 25
 Kaluzny, J. et al. 2005, *Proc. AIP*, 752, 70
 Kaluzny, J., Thompson, I. B., Rożyczka, M., Pych, W. & Narloch, W. 2014, *Acta Astron.*, 64, 309
 Kaluzny, J., Thompson, I. B., Dotter A., Rożyczka, M., Schwarzenberg-Czerny A., Burley G.S., Mazur B., Rucinski S.M., 2015, *AJ*, 150, 155
 Kolenberg et al., 2010, *ApJ*, 713, L198
 Kovács G., 1998, *Mem. Soc. Astron. Ital.*, 69, 49
 Kovács G., 2016, *Comm. Konkoly Obs.*, 105, 61
 Kunder A., Stetson P.B., Catelan M., Walker A.R., Amigo P., 2013, *AJ*, 145, 33
 Kurtz D.W., et al., 2016, *MNRAS*, 455, 1237
 Mackey A.D., van den Bergh S., 2005, *MNRAS*, 360, 631
 Mazur, B., Kaluzny, J., & Krzeminski, W. 1999, *MNRAS*, 306, 727
 Molnár L., et al., 2015, *MNRAS*, 452, 4283
 Moskalik P., Kołaczowski Z., 2009, *MNRAS*, 394, 1649
 Moskalik P. et al., 2015, *MNRAS*, 447, 2348
 Netzel H., Smolec R., 2016, *Proc. Pol. Astron. Soc.*, 3, 36
 Netzel H., Smolec R., Dziembowski W., 2015, *MNRAS*, 451, L25
 Netzel H., Smolec R., Moskalik P., 2015a, *MNRAS*, 447, 1173
 Netzel H., Smolec R., Moskalik P., 2015b, *MNRAS*, 453, 2022
 Nowakowski R., Dziembowski W., 2001, *Acta Astron.*, 51, 5
 Olech A., Moskalik P., 2009, *A&A*, 494, L17
 Olech, A., Kaluzny, J., Thompson, I. B., Pych, W., Krzeminski, W., & Schwarzenberg-Czerny, A., 1999, *AJ*, 118, 442
 Olech, A., Kaluzny, J., Thompson, I. B., Pych, W., Krzeminski, W., & Schwarzenberg-Czerny, A., 2001, *MNRAS*, 321, 421
 Poleski R., 2008, *Acta Astron.*, 58, 313
 Poretti E., 2001, *A&A*, 371, 986
 Poretti E., et al., 2005, *A&A*, 440, 1097
 Simon N.R., Clement C.M., 1993, *ApJ*, 410, 526
 Skarka M., 2013, *A&A*, 549, 101
 Smolec R., 2016, *Proc. Pol. Astron. Soc.*, 3, 22
 Smolec R., Śniegowska M., 2016, *MNRAS*, 458, 3561
 Smolec R. et al., 2015, *MNRAS*, 447, 3756

- Smolec R., Prudil Z., Skarka M., Bakowska K., 2016, *MNRAS*, 461, 2934
 Soszyński I., et al., 2010, *Acta Astron.*, 60, 17
 Soszyński I., et al., 2014, *Acta Astron.*, 64, 177
 Soszyński I., et al., 2016, *MNRAS*, 463, 1332
 Szabó R. et al., 2010, *MNRAS*, 409, 1244
 Szabó R., Benkő J.M., Páparó M., 2014, *A&A*, 570, A100
 Szeidl B., Hurta Zs., Jurcsik J., Clement C., Lovas, M., 2011, *MNRAS*, 411, 1744
 Zloczewski K., Kaluźny J., Rożyczka M., Krzeminski W., Mazur B., 2012, *Acta Astron.*, 62, 357

SUPPORTING INFORMATION

Additional Supporting Information may be found in the online version of this article:

AnimationV5 – Animation shows light curve changes over the Blazhko cycle for V5.

AnimationV10 – Animation shows light curve changes over the Blazhko cycle for V10.

AnimationV31 – Animation shows light curve changes over the Blazhko cycle for V31.

This paper has been typeset from a $\text{\TeX}/\text{\LaTeX}$ file prepared by the author.